

A Bird's Eye View of Nonlinear System Identification

Luis A. Aguirre

Departamento de Engenharia Eletrônica
 Programa de Pós-Graduação em Engenharia Elétrica
 Universidade Federal de Minas Gerais — Av. Antônio Carlos 6627,
 31270-901 Belo Horizonte MG, Brazil
 aguirre@ufmg.br

Abstract

This text aims at providing a bird's eye view of system identification with special attention to nonlinear systems. The driving force is to give a feeling for the philosophical problems facing those that build mathematical models from data. Special attention will be given to grey-box approaches in nonlinear system identification. In this text, grey-box methods use auxiliary information such as the system steady-state data, possible symmetries, some bifurcations and the presence of hysteresis. The text ends with a sample of applications. No attempt is made to be thorough nor to survey such an extensive and mature field as system identification. In most parts references will be provided for a more detailed study.

Contents

1	Introduction	2
2	Testing and Data Collection	4
2.1	Testing	4
2.2	Choosing the sampling period	7
3	Choice of Model Class	8
4	Structure Selection	11
4.1	The ERR, SRR and SSMR criteria	12
4.2	Other criteria	13

5	Parameter Estimation	15
5.1	Underlying issues	16
5.2	Classical estimators	19
5.3	The danger of overparametrization	21
6	Model Validation	22
6.1	Residual tests	23
6.2	Dynamical invariants	23
6.3	Synchronization	24
7	Grey-Box Techniques	25
7.1	\mathcal{I} is the static function	26
7.2	\mathcal{I} is steady-state data	28
7.2.1	Constraining parameters	29
7.2.2	Imposing a transcritical bifurcation	30
7.2.3	Biobjective parameter estimation	33
7.3	Other types of auxiliary information	35
8	Examples and Case Studies	37
8.1	Pneumatic valve with hysteresis	37
8.2	Dynamical and steady state data from an oil well	41
8.3	Imposing equilibria to model vector fields	46
8.3.1	The challenge	46
8.3.2	The methodology	47
8.3.3	Benchmarks	50
9	Further Reading	52

1 Introduction

System identification is the “art” of building dynamical mathematical models from data, which are measured from a system which, in principle, could be any dynamical system. A typical system identification problem can be divided into five steps: i) testing and data collection, ii) choice of model class, iii) structure selection, iv) parameter estimation and v) model validation. One of the aims of this text is to provide some preliminary discussion to each of these steps, with a clear bias towards nonlinear system identification. Black-box and grey-box techniques will be mentioned.

In doing this, a somewhat “philosophical framework” will be proposed in order to bring home to the newcomer some of the real challenges of this fascinating field. Such a framework is admittedly subjective, but it is believed that it will prove helpful in understanding a few important problems and fundamental challenges in system identification.

The statement of a system identification problem is simple and can be declared thus (see Figure 1): given a dynamical system \mathcal{S} , possibly nonlinear, from which a set of measured data Z^N is available, find a mathematical model \mathcal{M} that represents \mathcal{S} in some meaningful way. To build \mathcal{M} exclusively from Z^N is a *black-box identification problem*. In *grey-box problems*, besides Z^N there will be some other source of information about \mathcal{S} . In Z^N , N indicates the length of the data set and will be omitted in general.¹

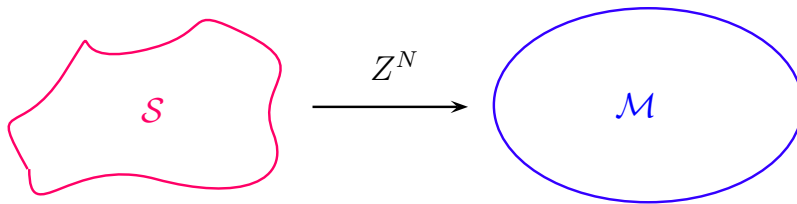


Figure 1: Simplified schematic diagram for black-box identification, where \mathcal{S} represents the system that should be approximated by a model \mathcal{M} which is built from a set of measured data Z^N of length N .

The following points should be noticed:

1. in black-box system identification, because Z is all there is to build \mathcal{M} , all relevant information about \mathcal{S} should be in such data. Hence, Z has to be carefully obtained;
2. the model \mathcal{M} must be a member of a model class \mathcal{M}^c that should be consistent with the relevant aspects of \mathcal{S} that are aimed at. For instance, if \mathcal{S} is dynamical and nonlinear, so must be \mathcal{M}^c ;
3. given a class of models \mathcal{M}^c consistent with \mathcal{S} and the modelling aims, there are many specific candidate models, i.e. $\{\mathcal{M}_1, \mathcal{M}_2 \dots \mathcal{M}_n\} \in \mathcal{M}^c$ which are not equivalent nor necessarily adequate to represent specific features of \mathcal{S} ;

¹Some authors restrict grey-box problems to that of estimating parameters of an equation that comes from first principles.

4. a parametric model \mathcal{M} is composed by variables and parameters which must be chosen and estimated;
5. a mathematical model \mathcal{M} is not directly comparable to a physical system \mathcal{S} , because they are entities of different natures. How can one decide if \mathcal{M} represents \mathcal{S} ?

The five aspects just mentioned are closely related to the five steps of a typical identification problem, listed in the opening paragraph. In general terms, this text will be organised in two parts. First, each of the aforementioned five steps will be briefly introduced. This is done in Sections 2 to 6. In the second part, some specific aspects, especially related to grey-box techniques will be presented in Section 7. Section 8 discusses three case studies in order to illustrate some of the main ideas. The work concludes with suggestions for further reading.

2 Testing and Data Collection

There are a number of situations in system identification in which one must build the model from historical data. By historical data it is meant data that have been collected not as a result of any specific designed test. For now, we will assume that a specific test can be performed to produce Z . Before we start it will be convenient to point out that the data are very often composed by inputs \mathbf{u} and outputs \mathbf{y} . For now, we will restrict ourselves to the SISO (single-input single-output) case, hence $Z^N = [u(k) \ y(k)]$, $k = 1, 2, \dots, N$.

The standard situation in system identification is that both \mathcal{S} and therefore \mathcal{M} are dynamical. Hence, it is necessary that Z be produced as a result of a dynamical test on \mathcal{S} . That is, the input $u(k)$ is designed in such a way that the relevant dynamics of \mathcal{S} appear in $y(k)$. A fundamental point here is to realize that because \mathcal{M} is built exclusively from Z (the black-box case), features of \mathcal{S} that do not show up in Z will most likely not appear in \mathcal{M} either. In discussing this point, it will be convenient to address the linear and nonlinear cases in turn.

2.1 Testing

Every physical system \mathcal{S} is typically nonlinear and time-varying. Let us assume that the intended model \mathcal{M} is linear. This means to say that we are

interested in the linear aspects of the dynamical behaviour of \mathcal{S} . Hence Z must be consistent with such an aim. In order to guarantee this and avoid that nonlinear features of \mathcal{S} appear in Z , a typical test is to excite \mathcal{S} around an operating point, that is to say, that the amplitude range of $u(k)$ must be limited to a region in which “the nonlinearities of \mathcal{S} are not excited”.

Also, because \mathcal{M} is intended to be dynamical, Z must have such information. If $u(k)$ is too slow, the system \mathcal{S} will not have any troubles in following the input and the dynamics will not appear in $y(k)$. When a driver slows down before passing a speed bump the idea is *not* to excite the dynamics of the vehicle suspension. So, in general, slow input signals result in data with poor dynamical information. On the other extreme the practitioner also faces problems. If the input is too fast, then there is not enough time for the system to react to the input changes and there is no significant energy transfer from the input to the system. In such a situation the data also turn out to be poor from a dynamical point of view. In technical terms, the power spectrum of the input $\Phi_u(\omega) = \mathcal{F}(R_u)$ ² must have sufficient power in the frequency range of interest, that is, in the frequency range of the dominant dynamics of \mathcal{S} . If $\Phi_u(\omega)$ is nonzero at n frequencies, then $u(k)$ is said to be *persistently exciting of order n* . In practice, a signal is said to be persistently exciting if it is sufficiently rich in order to facilitate the estimation process.

Because \mathcal{M} should be time-invariant and \mathcal{S} is time-varying, one should guarantee that the time-varying aspect does *not* appear in Z . This is typically achieved by performing dynamical tests that are not too long. In other words, the changes in \mathcal{S} during the test should be negligible. The newcomer to the theory of dynamical systems should be aware that supposing a time-invariant system does *not* imply a constant output.

What changes if we aim at a nonlinear model? In what concerns the time-varying aspect of \mathcal{S} nothing changes because we still aim at a time-invariant model \mathcal{M} . Hence the period during which the data Z are collected still needs to be sufficiently short as to guarantee that it is reasonable to consider that \mathcal{S} did not change significantly during that period.

Because \mathcal{M} is now nonlinear, then it is required that the relevant nonlinear aspects of \mathcal{S} be present in Z . Clearly, the test cannot possibly be performed as for the linear case, on the contrary, a typical test for nonlinear

² \mathcal{F} denotes de Fourier transform and R_u is the covariance matrix of $u(k)$. The power spectrum of a signal is defined as the Fourier transform of the covariance matrix of such a signal.

system identification will probably specify large variations in the input signal $u(k)$ in order to excite the nonlinearities of \mathcal{S} and guarantee that they appear in the data Z . From a practical point of view, it is often difficult and unsafe to drive the system \mathcal{S} over a wide range of operating conditions. This is one of the practical challenges faced by the practitioner that aims at building nonlinear models from data. Fortunately, there are possibilities that help to face such challenges. A common one is to perform several low amplitude tests over a set of operating points that cover the region of interest. The inconvenience of this is that the test can turn out to be long. In Section 7.2 we will discuss another solution to this problem based on grey-box techniques.

If from an amplitude point of view the testing of nonlinear systems is more challenging than for linear systems, in terms of frequency content of the input, nonlinear systems are somewhat easier. The reason for this is that nonlinear systems transfer spectral power among different frequencies, which does *not* happen in linear systems. To see this, suppose we choose as input $u(k) = A \cos(\omega_0 t)$ with a sufficiently small value of A in order not to excite the nonlinearities in \mathcal{S} . Linear systems theory tells us that in steady-state the output will be of the form $y(k) = a_0 \cos(\omega_0 t + \phi_0)$. In other words, the gain at frequency ω_0 is a_0/A and the phase at that frequency is ϕ_0 (usually a negative value). That is we have identified the Bode diagram (frequency response) of \mathcal{S} only at ω_0 . Now it should become clear why $u(k)$ should be persistently exciting of large order n : to have information at n different frequencies.

Suppose that A is increased in order to excite the nonlinearities. Figure 2 shows both the input and output for this case. Clearly, the output has more than one frequency. This is a direct consequence of nonlinearity. Hence, in the case of nonlinear systems there is somewhat less strain on the test in what concerns frequency content of the input. A simple summary of this discussion is: for linear models input amplitudes should be low and the spectrum should be wide; for nonlinear models the amplitude profile should be large whereas the input spectrum can sometimes be narrow.

As a final remark in this section, what if we only have historical data in hand? The same principles apply, but now instead of performing a test to measure Z with the desired features, one must go through all the available data and find windows that present the desired characteristics. Such windows are candidates to compose Z . Procedures for detecting transients from a historical record can be found in (Ribeiro and Aguirre, 2015; Bittencourt et al., 2015).

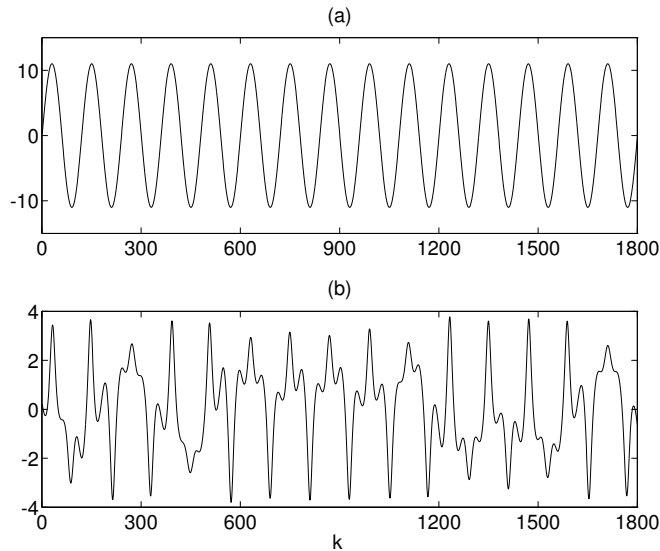


Figure 2: Simulated data from the Duffing-Ueda oscillator $\ddot{y} + 0.1\dot{y} + y^3 = u(t)$ for input (a) $u(t) = 11 \cos(t)$, and (b) output $y(t)$. Notice how $y(k)$ has many other frequencies besides $\omega = 1$ rad/s. That is due to nonlinearity.

2.2 Choosing the sampling period

When it comes to choosing the sampling time T_s , one immediately thinks in terms of Shannon's sampling theorem: a signal that does *not* have any components of frequency above $f_{\max} = 1/2T_s$ can be unambiguously reconstructed from a set of samples regularly spaced in time by T_s . In many practical problems, including system identification, this result is not totally practical for a couple of reasons. First and foremost, f_{\max} is generally not known beforehand, second, to sample a signal with a frequency just above $2f_{\max}$ is a lower bound rather than a comfortable working value.

On the other hand someone might suggest oversampling the data. This also has its troubles as consecutive samples are highly redundant and therefore the numerical problems that must be solved typically become ill-conditioned. A practical procedure that works well in many situations is the following. First, using an admittedly short sampling time record an over-sampled data set $Z^* = [u^*(k) \ y^*(k)]$, $k = 1, 2, \dots$. Now we want to choose a decimation factor $\Delta \in \mathbb{N}$ such that $u(k) = u^*(\Delta k)$ and $y(k) = y^*(\Delta k)$. It is assumed that all signals are band-limited.

First, the following covariance functions are computed

$$\begin{aligned} r_{y^*}(\tau) &= \text{E} \left[(y^*(k) - \overline{y^*(k)})(y^*(k - \tau) - \overline{y^*(k)}) \right] \\ r_{y^{*2}}(\tau) &= \text{E} \left[(y^{*2}(k) - \overline{y^{*2}(k)})(y^{*2}(k - \tau) - \overline{y^{*2}(k)}) \right], \end{aligned} \quad (1)$$

where $\text{E}[\cdot]$ indicates the mathematical expectation and the overbar indicates time-average. The first expression in (1) is the standard linear covariance function, whereas the second is a nonlinear function. Notice that such functions are computed using the oversampled data.

Second, plot functions $r_{y^*}(\tau)$ and $r_{y^{*2}}(\tau)$. Call τ_{y^*} $\tau_{y^{*2}}$ the lags at which the first minimum of each function occurs. Choose the least of them, that is $\tau_m^* = \min[\tau_{y^*}, \tau_{y^{*2}}]$. Call τ_m the corresponding value for the data decimated with factor Δ . Hence, we wish to determine Δ such that

$$10 \leq \tau_m \leq 20, \quad (2)$$

where the limits can sometimes be relaxed to 5 and 25.

For example, consider an oversampled signal $y^*(k)$ for which the linear and nonlinear covariance functions are shown in Figure 3. The smallest lag corresponding to the first minimum is $\tau_m^* = 55$, hence if we choose $\Delta = 4$, this value for the decimated signal will be $\tau_m \approx 14$, which satisfies (2). Hence the decimation factor could be $\Delta = 4$. As a final remark, it should be carefully noticed that if the data Z is composed of more than one signal, the decimation factor applied must be the same for all signals. Therefore, the Δ used must be the smallest that will satisfy the decimation criterion for all signals.

Some technical aspects of testing can be found in (Leontaritis and Billings, 1987a; Gevers et al., 2009) and specifically for closed-loop systems in (Bombois et al., 2006). The decimation criterion discussed in this section was originally put forward in (Aguirre, 1995) and some effects on aspects of system identification have been discussed in (Billings and Aguirre, 1995).

3 Choice of Model Class

This is probably the step which receives less attention and it is not really difficult to see why. From a more technical point of view, it suffices that the model class \mathcal{M}^c be sufficiently general to include the relevant aspects of

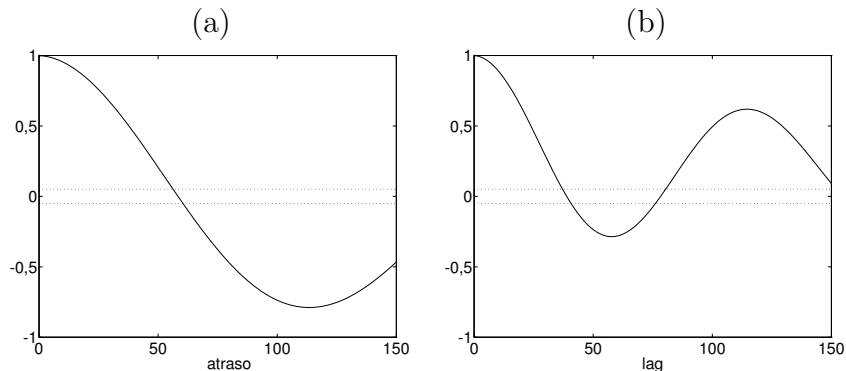


Figure 3: Autocovariance functions for an oversampled signal $y^*(k)$: (a) $r_{y^*}(\tau)$ and (b) $r_{y^*2'}(\tau)$. In this example $\tau_m^* = \min[\sim 115, \sim 55] = 55$. Plot (a) was obtained using the x variable of Chua’s oscillator, and plot (b) with the y variable of the same system. This shows that an acceptable samplint time for the x variable would result in undersampling the y variable. See (Aguirre, 1995) for details.

S. From a practical point of view, the practitioner tends to use the model class that he/she is familiar with. Can we be more specific and “scientific” in choosing the model class?

Probably the most important choice is to decide if \mathcal{M}^c will be linear or not. This of course has to do with the intended use of the model. For instance, although linear models are admittedly less effective in representing systems in general, they could be preferred, say, for control purposes. Within the class of linear models, there are some subclasses as, for instance, transfer functions and state space representations. If a model is intended to implement a Kalman filter, then \mathcal{M}^c is likely to be the class of linear models in state-space form (Van Overschee and De Moore, 1996; Borjas and Garcia, 2011).

In the realm of nonlinear model classes, the variety is very large, in what follows only a few are mentioned: Volterra series (Campello et al., 2006), nonlinear output frequency response functions (Bayma et al., 2018), Hammerstein and Wiener models (Bai, 2002; Aguirre et al., 2005a; Schoukens and Tiels, 2017). These model classes have been surveyed in (Billings, 1980). Polynomial and rational NARMAX (nonlinear autoregressive moving average models with exogenous variables) (Leontaritis and Billings, 1985; Billings and Chen, 1989; Billings and Zhu, 1991). A recent overview of such model classes and related methods can be found in (Billings, 2013). Differential equations

(continuous-time models) have been used in (Gouesbet and Letellier, 1994; Mangiarotti et al., 2012), radial-basis functions (Chen et al., 1990a; Ogawa et al., 1996) and neural networks (Narendra and Parthasarathy, 1990; Chen et al., 1990b; Billings and Chen, 1992; Ballini and Gomide, 2002; Forgione and Piga, 2021). See (Rocha and Serra, 2017) and references therein for a description of NARX neuro-fuzzy models. The main motivation for using such nonlinear representations is that they are universal approximations, hence regardless of the features of \mathcal{S} , such model classes are sufficiently general to represent the system.

The model classes mentioned in the previous paragraph can be classified as global in the sense that a single model structure is used to map the whole set of inputs to the outputs. On the other extreme, one finds models formed by a combination of linear models that are responsible for representing the data only locally (Barreto and Souza, 2016; Barbosa et al., 2018; Liu et al., 2019). See (Johansen and Foss, 1993; Göttsche et al., 1998) for some early works on this topic. An intermediary class is that of regional models (Souza Junior et al., 2015).

Although several of such representations can be considered fairly general, the difficulty of using them in practical problems may vary greatly, as will be pointed out later. Also, in Section 7 it will be argued that the model class can be chosen based on the ease with which auxiliary information can be used in the process of model building. This will prove to be one of the few objective criteria available for choosing the model class.

In order to facilitate discussions about structure selection and parameter estimation, it will be convenient to choose a working model class. Although most of what will be said is applicable to any model class, in what follows we shall consider the class of NARMAX models (Chen and Billings, 1989)

$$y(k) = F^\ell[y(k-1), \dots, y(k-n_y), u(k-d), \dots, u(k-n_u), e(k-1), \dots, e(k-n_e), e(k)], \quad (3)$$

where $e(k)$ accounts for uncertainties and possible noise. Also n_y , n_u and n_e are the maximum lags in each variable, and $d \geq 1$ is the pure delay. The function F can be any nonlinear function, such as a neural network, radial basis function, rational or polynomial, each of which determines a different model class. For the sake of discussion, in what follows $F^\ell[\cdot]$ will be a polynomial with nonlinearity degree ℓ . To estimate the pure delay d is both important and challenging in the context of system identification (Alves et al., 2017).

4 Structure Selection

Having decided which model class to use, it is important to realize that there are scores of different model structures within the chosen class \mathcal{M}^c , that is $\{\mathcal{M}_1, \mathcal{M}_2 \dots \mathcal{M}_n\} \in \mathcal{M}^c$, where n can be very large. On its own that remark justifies the search for a much smaller set of model structures that should be considered in a given situation. However the problem is indeed far more critical than what it seems at first sight. If the model class \mathcal{M}^c is very general, the temptation to grow the model more than needed is great. This is known in the literature as *overparametrization* or *overfitting* and has severe detrimental effects on the dynamics of the identified models (Aguirre and Billings, 1995a). In this section we will provide a brief discussion for model classes that are linear-in-the-parameters to give the reader a feel for the problem. In the next section it will be explained why it is relatively “natural” to overparametrize a model.

We start by assuming that \mathcal{M}^c is the class of single-output NARX polynomials. Hence, the corresponding model – see (3) – can be rewritten as:

$$\begin{aligned} y(k) &= \theta_1 \psi_1 + \theta_2 \psi_2 + \dots + \theta_{n_\theta} \psi_{n_\theta} + e(k) \\ &= [\psi_1 \ \psi_2 \ \dots \ \psi_{n_\theta}] \boldsymbol{\theta} + e(k) = \boldsymbol{\psi}(k-1)^T \boldsymbol{\theta} + e(k) \end{aligned} \quad (4)$$

where ψ_i is the i th regressor and θ_i the corresponding parameter which can be written in vector form as $\boldsymbol{\theta} = [\theta_1 \ \theta_2 \ \dots \ \theta_{n_\theta}]^T$. The (column) vector of regressors is $\boldsymbol{\psi}(k-1)$, indicating that all regressors are taken at most up to instant $k-1$. The regressors are any combinations up to degree ℓ of input and/or output variables down to lags n_u and n_y , respectively. For instance, $\psi_1 = y(k-1)$, $\psi_2 = u(k-3)$ and $\psi_3 = y(k-1)u(k-2)^2$ are possible regressors for $n_y = n_u = \ell = 3$.

Hence, the regressors of model (4) may contain any combination of lagged inputs, outputs and noise terms up to degree ℓ . The number of such combinations is determined by the values of ℓ , n_y , n_u and n_e and can easily include thousands of candidate regressors. This huge amount of terms is a major impediment to the usefulness of the estimated model and some kind of mechanism is called for in order to automatically choose the best n_θ regressors to compose the model. This problem is often referred to as *model structure selection* and must be judiciously accomplished regardless of the mathematical representation being used.

This model class is said to be linear-in-the-parameters because all the known parameters can be separated from the known regressors, as seen in (4).

In the case of model classes that are not linear in the parameters, typically we would find unknown parameters in $\boldsymbol{\psi}(k-1)$. The fact that a model be linear-in-the-parameters does not mean that it satisfies the superposition principle, on the contrary. Many linear-in-the-parameters model classes are strongly nonlinear.

4.1 The ERR, SRR and SSMR criteria

Because of their usefulness and wide acceptance, two criteria for choosing the regressors of NARX polynomial models are briefly described next.

A widely used criterion in the structure selection is the *error reduction ratio* (ERR) (Billings et al., 1989). This criterion, which is based on one-step-ahead prediction error minimization, evaluates the importance of the model terms according to their ability to explain the output variance.

The reduction in the variance of the residuals, that occurs as new terms are included in the model, can be normalized in relation to the output variance σ_y^2 . Then, the error reduction ratio due to the inclusion of the i th regressor in the model can be written as:

$$\text{ERR}_i = \frac{\text{MS1PE}(\mathcal{M}_{i-1}) - \text{MS1PE}(\mathcal{M}_i)}{\sigma_y^2}, \quad i = 1, 2, \dots, n, \quad (5)$$

where $\text{MS1PE}(\mathcal{M}_i)$ stands for the mean square one-step-ahead (OSA) prediction error of the model with i terms (regressors); n is the number of candidate terms tested for; and \mathcal{M}_i represents a family of models with nested structures, thus $\mathcal{M}_{i-1} \subset \mathcal{M}_i$. In (5) the numerator equals the reduction in variance of the residuals due to the inclusion of the i th regressor.

A somewhat related criterion, called *simulation error reduction ratio* (SRR), was defined in (Piroddi and Spinelli, 2003) as:

$$\text{SRR}_i = \frac{\text{MSSE}(\mathcal{M}_{i-1}) - \text{MSSE}(\mathcal{M}_i)}{\sigma_y^2}, \quad i = 1, 2, \dots, n, \quad (6)$$

where $\text{MSSE}(\mathcal{M}_i)$ stands for the mean square simulation error of the model with i terms (regressors). In (6) the *free-run* simulation is used. In Sec. 5 the important difference between OSA prediction and simulation errors will be pointed out.

In the same vein, the *simulation similarity maximization rate* was proposed as (Araújo et al., 2019):

$$\text{SSMR}_i = \frac{\hat{V}_\sigma(y, \hat{y}_{i+1}) - \hat{V}_\sigma(y, \hat{y}_i)}{\sigma_y^2}, \quad i = 1, 2, \dots, n, \quad (7)$$

where \hat{y}_i is the free-run simulated output of the current model and \hat{y}_{i+1} refers to the model that has the same regressors as the one that produced \hat{y}_i with the addition of the regressor that is being tested and n is the number of candidate regressors. In (7) $\hat{V}_\sigma(X, W)$ is the correntropy between the random variables X and W and quantifies the average similarity between them.

The SRR, is effective in non ideal identification conditions and often yields more compact models. On the other hand, such a criterion requires a significantly greater computational effort as it will be discussed in Section 5. To partially circumvent such a limitation alternative procedures have been proposed (Bonin et al., 2010; Farina and Piroddi, 2010). The SSMR, as the SRR, benefits from using free-run simulated model outputs. Also, it is less sensitive to eventual problems caused by non-Gaussianity which is the norm in the nonlinear context.

See (Mendes and Billings, 2001; Wei et al., 2004; Hong et al., 2008; Piroddi, 2008; Wei and Billings, 2008; Alves et al., 2012; Martins et al., 2013; Gu and Wei, 2018) for a comparison of methods and some recent techniques on structure selection approaches somewhat related to the ERR, SRR and SSMR methods.

4.2 Other criteria

Twin concepts that were developed to aid in structure selection problems are the *term clusters*, indicated by $\Omega y^p u^m$, and the respective *cluster coefficients*, by $\Sigma y^p u^m$. Terms of the form $y^p(k - \tau_j)u^m(k - \tau_i) \in \Omega_{y^p u^m}$ for $m+p \leq \ell$, where τ_i and τ_j are any time lags. For instance, for the model $y(k) = \theta_1 y(k-1)y(k-2) + \theta_2 y(k-1)u(k-2) + \theta_3 y(k-3)u(k-3)$ we have $n_y = n_u = 3$, $d = 2$, $\ell = 2$. This model has two term clusters, namely: Ω_{y^2} with coefficient $\Sigma_{y^2} = \theta_1$ and Ω_{uy} with coefficient $\Sigma_{uy} = \theta_2 + \theta_3$.

Often the coefficients of spurious term clusters become very small or oscillate around zero as the model increased in size, hence this could be used to aid in detecting the order of linear models (Aguirre, 1994) or to detect and discard term clusters in nonlinear system identification (Aguirre and Billings,

1995b; Aguirre et al., 1997). Later on, these concepts turned out to be very useful in grey-box identification problems, as will be discussed later.

The use of correlation test has been discussed in (Stoica et al., 1986; Leontaritis and Billings, 1987b), but the procedure is less specific than what one would like.

In *semiphysical modeling* prior knowledge of the system is used to establish suitable, though usually nonlinear, terms of the measurements in order to improve on the model structure (Lindskog and Ljung, 1995). In other words, in *semiphysical modeling* physical insight of the system being modeled is used to determine key term clusters. Of course, *semiphysical modeling* falls into the category of grey-box techniques.

Following a probabilistic framework, the Randomized algorithm for Model Structure Selection (RaMSS) was proposed recently (Falsone et al., 2015). The method was formulated for the NARX polynomial model class and extended to cope with NARMAX polynomial model class in (Retes and Aguirre, 2019). The main idea of this approach is to start with a tentative probability distribution over regressors, e.g. a uniform distribution indicating that all regressors start having the same probability of composing the model. Using such distribution sample models are produced and tested. Regressors that compose good models have their probability increased whereas regressors of poorly performing models have a smaller probability of being chosen in future samples after several iterations, the best regressors have a high probability whereas bad regressors have small or even null probability. In the original RaMSS algorithm the regressors are dealt with independently. A more refined approach that takes into account possible relationships among regressors has been developed in (Bianchi et al., 2017). In short, in the last reference the inclusion of a regressor in a model is based on the previously selected regressors. This does not mean that the model is built in a forward regression style, because regressors can be discarded from the model.

The bias/variance dilemma, originally discussed in the context of neural networks (Geman et al., 1992), is useful for understanding the pros and cons of *slight* overparametrization. Such a dilemma underlines several so called *information criteria* such as Akaike’s criterion (Akaike, 1974). These criteria are helpful to decide the size of a model. Hence, ERR, SRR and SMRR criteria help rank regressors according to their importance but usually a different criterion is needed to decide where to stop including terms into the model. A very interesting feature has been reported concerning the bias/variance dilemma for network models (Belkin et al., 2019). In short,

strongly overparameterized models – models with a number of features (independent terms) that greatly exceeds the number of data in the training set – eventually experience a second decrease in the mean squared prediction error. This is called the second “descent” and has not only been verified in some classification problems but also in modeling dynamics (Ribeiro et al., 2021). The generality of such results still needs to be established but so far they seem to apply in network-type models for which it is viable to easily increase the number of features used by the model.

By explicitly including the number of model terms, thus increasing the learning dimension, Hafiz and co-workers have used particle swarm algorithms to address the problem of structure selection in nonlinear system identification (Hafiz et al., 2019).

The problem of determining the model structure clearly extends to other model classes. For instance, in the case of neural networks there is an extensive literature in *pruning* methods (Reed, 1993). The ERR has been adapted for choosing the centres of radial basis function networks (Chen et al., 1990a; Aguirre et al., 2007). As it will be discussed in Sec. 7, auxiliary information regarding fixed points and steady-state at large provides important clues for structure selection in the case of polynomial models.

In closing this section it is important to point out that for a set of data of limited size and quality there is more often than not more than one model structure that is compatible with the data (Barbosa et al., 2015), also see examples in (Falson et al., 2015; Avellina et al., 2017). Hence there is uncertainty not only on the model parameters, but also on the model structure. To quantify such uncertainty remains an open problem (Barbosa et al., 2015; Gu and Wei, 2018).

5 Parameter Estimation

By now we have chosen a model class \mathcal{M}^c and a specific model structure within that class. Of course, in practice we usually choose more than a model structure to work with, but for the sake of argument, let us focus on a single model structure. As seen in (4) the model is composed by a structure (regressor variables ψ_i) and parameters that are grouped in a vector $\boldsymbol{\theta}$. Hence our model can be represented as $\mathcal{M}(\boldsymbol{\theta})$ and now the last aspect of the model that still needs determining is $\boldsymbol{\theta}$. In what follows some of the challenges that must be faced in estimating $\boldsymbol{\theta}$ will be discussed before mentioning some

classical estimators.

5.1 Underlying issues

As in Sec. 1, we start with a philosophical discussion which hopefully will prove helpful. In a very loose and intuitive way, we can say that both the structure of \mathcal{M} and its parameters θ should be chosen such that the estimated model $\mathcal{M}(\hat{\theta})$ be a good representation of the system \mathcal{S} . The hat on $\hat{\theta}$ indicates that it is an estimated value of θ .

Since we assume that at this stage the model structure has been chosen, we move on to estimate the parameters. Hence we could imagine a naïve procedure by which we chose the vector $\hat{\theta}$ that best approximates the model to the system, that is, $\mathcal{M}(\hat{\theta}) \equiv \mathcal{S}$. As mentioned before, this is not a viable problem because model and system are of a very different nature. One is a set of equations the other is a set of devices and e.g. physical or biological components, depending on the system. Hence to move towards a solution, we measure from the system \mathcal{S} a set of data Z , but this is still not sufficient because, for the same reason as before, we cannot compare a model to data, that is, to search for $\hat{\theta}$ such that $\mathcal{M}(\hat{\theta}) \equiv Z$ is *not* a viable problem either. So, in order to come up with a viable problem, we produce data using the model $Z_{\mathcal{M}(\hat{\theta})}$ – which will be indicated as $Z_{\mathcal{M}}$ for short – and now it is possible to compare data with data, because these are of the same nature. Hence, we search for $\hat{\theta}$ such that $Z_{\mathcal{M}}$ is as close to Z as possible.

A standard and convenient way of measuring how close a signal is from another is to compute the sum of squared errors:

$$J = \sum_{k=1}^N [y(k) - \hat{y}(k)]^2, \quad (8)$$

where $y(k)$ is the measured output and $\hat{y}(k)$ is the model output produced with $\hat{\theta}$. Therefore J indirectly depends on $\hat{\theta}$, because $\hat{y}(k)$ does. Because $Z = [u(k) \ y(k)]$, $k = 1, \dots, N$ and $Z_{\mathcal{M}} = [u(k) \ \hat{y}(k)]$, $k = 1, \dots, N$ (notice that $u(k)$ must be the same in both data sets), for the sake of discussion (8) will be represented as $J(Z, Z_{\mathcal{M}})$. In this framework, if the data sets are similar then $J(Z, Z_{\mathcal{M}})$ is “small”. Or, in other words, the smaller $J(Z, Z_{\mathcal{M}})$ the closer the data sets Z and $Z_{\mathcal{M}}$ are.

A remaining key issue is to decide in which way the model will be used to produce the data $Z_{\mathcal{M}}$. We consider two different ways of doing so by

means of a specific and simple example. Consider the model for which the parameters are assumed known

$$\hat{y}(k) = [y(k-1) \ u(k-1) \ y(k-1)u(k-1)]\hat{\theta}, \quad (9)$$

hence the right hand side is completely known and, therefore, so is the model output $\hat{y}(k)$. For example, the model output at time $k = 10$ is given by model (9) as:

$$\hat{y}(10) = [y(9) \ u(9) \ y(9)u(9)]\hat{\theta},$$

where $y(9)$ is the 9th measured sample of the output, and so on. Because we feed the model with *measured* data and use it just to move one-step-ahead, the output computed this way is called *one step ahead* (OSA) prediction and will be indicated by $\hat{y}_1(k)$

A different value of $\hat{y}(10)$ would be obtained if, *using the same model*, we compute

$$\hat{y}(10) = [\hat{y}(9) \ u(9) \ \hat{y}(9)u(9)]\hat{\theta},$$

where,

$$\hat{y}(9) = [\hat{y}(8) \ u(8) \ \hat{y}(8)u(8)]\hat{\theta},$$

and so on. Because this second procedure feeds the model with previously simulated values, the output is often referred to as *simulated* or *free-run* output and will be indicated by $\hat{y}_s(k)$. The reader will immediately realize that the ERR criterion is based on $\hat{y}_1(k)$ and the SRR and SMRR, on $\hat{y}_s(k)$, see Sec. 4.1.

What are the main differences between $\hat{y}_1(k)$ and $\hat{y}_s(k)$? Both outputs are produced by the same model and we can think of the data revealing or accumulating “model signatures” or “model features”. Because to produce $\hat{y}_1(k)$ the model only has to predict one step into the future starting from measured data, the model features are somewhat hard to recognize in $\hat{y}_1(k)$. Imagine that the model is unstable, of course the model divergence will be in $\hat{y}_1(k)$ when compared to $y(k)$, but – especially if the sampling time is short – that divergence may not be significant. On the other hand, because $\hat{y}_s(k)$ is produced from previously simulated output, the model features will tend to accumulate in such data which, in a sense, will be far more informative about the model. So, if the model is unstable, $\hat{y}_s(k)$ will diverge to infinity.

From the previous discussion there should be no doubts that $\hat{y}_s(k)$ is advantageous over $\hat{y}_1(k)$ from a dynamical point of view. Hence it would be nice if we could use the data $Z_{\mathcal{M}_s}$ instead of $Z_{\mathcal{M}_1}$ in estimating the parameter vector. Let us state this more formally in terms of two possible estimators that boil down to two optimization problems:

$$\hat{\boldsymbol{\theta}}_1 = \arg \min_{\boldsymbol{\theta}} J(Z, Z_{\mathcal{M}_1}) \quad (10)$$

and

$$\hat{\boldsymbol{\theta}}_s = \arg \min_{\boldsymbol{\theta}} J(Z, Z_{\mathcal{M}_s}). \quad (11)$$

For instance, the optimization problem in (10) is read thus: the estimated vector $\hat{\boldsymbol{\theta}}_1$ is the argument among all possible $\boldsymbol{\theta}$ that minimizes $J(Z, Z_{\mathcal{M}_1})$, and likewise for the problem in (11).

Since we have already seen that, from a dynamical point of view, $Z_{\mathcal{M}_s}$ is preferable to $Z_{\mathcal{M}_1}$, it seems natural to conclude that the estimator in (11) is probably preferable to the one in (10). Well, in fact, the estimator in (11) is indeed much more robust to noise and other aspects than (10) in many cases (Ribeiro and Aguirre, 2018). This kind of reasoning may underlie similar problems (Schoukens et al., 2021). However, the optimization problem in (11) is nonconvex, whereas the optimization problem in (10) is convex and can be solved in a much simpler way. Hence, to summarize, from a *dynamical* point of view, the solution to problem (11) is preferable, but at the cost of having to solve a nonconvex optimization problem. On the other hand to solve problem (10) is *numerically* preferable, although the solution $\hat{\boldsymbol{\theta}}_1$ might not be as good and as robust as $\hat{\boldsymbol{\theta}}_s$.

Let us close this discussion with three remarks. First, many of the “standard” recommendations in system identification about testing, input persistent excitation, choice of model structure and so on are made in order to improve the chances of $\hat{\boldsymbol{\theta}}_1$ – which is a numerically inexpensive solution – being such that the model $\mathcal{M}(\hat{\boldsymbol{\theta}}_1)$ is dynamically acceptable (Aguirre et al., 2010). In second place, it must be noticed that for model classes that are *not* linear-in-the-parameters, even problem (10) is a nonconvex optimization problem. Finally, parameters of chaotic systems can be estimated solving (10) because at such short single steps, the effect of the extreme sensitivity to initial conditions is not critical.

5.2 Classical estimators

In this section we start by presenting the least squares estimator, which is the classical solution to problem in (10), which applies to model classes that are linear-in-the-parameters. To see this we start considering the model structure in (4) and a set of data Z^N . We can now write (4) for any value of k within the data range. For instance, for $k = 10$ we can write $y(10) = \boldsymbol{\psi}(9)^\top \boldsymbol{\theta} + e(10)$ where $\boldsymbol{\psi}(9)$ is the vector of regressors which goes up to time $k - 1 = 9$ and $e(10)$ is whatever cannot be explained in the data at time $k = 10$ using $\boldsymbol{\psi}(9)^\top \boldsymbol{\theta}$. Hence we would like to find $\boldsymbol{\theta}$ in such a way as to minimize the unexplained part $e(10)$. In order to gain robustness, we consider the model structure (4) along all the data, which we now call the *identification data set* Z^N . That means that for each value of k within the data range we will have an equation of the form $y(k) = \boldsymbol{\psi}(k-1)^\top \boldsymbol{\theta} + e(k)$ which can be expressed as a matrix equation thus:

$$\mathbf{y} = \Psi \boldsymbol{\theta} + \mathbf{e}, \quad (12)$$

where $\Psi \in \mathbb{R}^{N \times n_\theta}$,³ $\boldsymbol{\theta} \in \mathbb{R}^{n_\theta}$ and $\mathbf{y} = \{y(k)\}_{k=1}^N$. Suppose we have an estimate of the parameter vector $\hat{\boldsymbol{\theta}}$. Then (12) can be rewritten as:

$$\begin{aligned} \mathbf{y} &= \Psi \hat{\boldsymbol{\theta}} + \boldsymbol{\xi}, \\ &= \hat{\mathbf{y}}_1 + \boldsymbol{\xi} \end{aligned} \quad (13)$$

where $\boldsymbol{\xi} = \{\xi(k)\}_{k=1}^N$ is the vector of *residuals* which can be taken as an estimate of the unknown noise \mathbf{e} under “favorable” conditions and $\hat{\mathbf{y}}_1$ is the vector of OSA predictions.

One way of determining $\hat{\boldsymbol{\theta}}$ if Ψ does not contain columns correlated with $\boldsymbol{\xi}$ (as in the case of NARX models) is by the Least-Squares (LS) estimator, that minimizes the mean squared value of $\boldsymbol{\xi} = \mathbf{y} - \hat{\mathbf{y}}_1$ and is given by

$$\hat{\boldsymbol{\theta}}_{\text{LS}} = (\Psi^\top \Psi)^{-1} \Psi^\top \mathbf{y}, \quad (14)$$

and is the solution to problem (10).

In the classical LS solution (14) all the residuals receive equal weight, that is $\xi(k) = y(k) - \hat{y}_1(k)$, $\forall k$. There might be reasons in some situations to give specific weights to the residuals as $w(k)\xi(k)$. Placing $w(k)$, $k = 1, \dots, N$ along the diagonal of a matrix $W \in \mathbb{R}^{N \times N}$, the solution

$$\hat{\boldsymbol{\theta}}_{\text{WLS}} = (\Psi^\top W \Psi)^{-1} \Psi^\top W \mathbf{y} \quad (15)$$

³In fact, because of the lags in the model, a data set of size N will result in slightly smaller set of equations. We will not detail this to keep nomenclature as light as possible.

is known as the weighted least squares estimator (WLS). There are two classical choices for W . If the weighting matrix is taken as the covariance matrix for the noise, the WLS becomes the so called Markov estimator which is akin to the generalized least squares estimator. A second important choice of W is to take the weight of the present moment as $w(k) = 1$, the previous one as $w(k-1) = \lambda$, then $w(k-2) = \lambda^2$ and so on, where $\lambda < 1$ is known as the forgetting factor. Hence the WLS estimator is useful to derive a recursive LS estimator with forgetting factor.

The optimization problems in (10) and (11) are said to be unconstrained. This means that all the degrees of freedom are used to minimize the functional J , and the solution can be any vector of real values $\hat{\boldsymbol{\theta}} \in \mathbb{R}^{n_\theta}$. Now suppose that there is a set of constraints on the parameter vector written as $\mathbf{c} = S\boldsymbol{\theta}$, where \mathbf{c} is a given constant vector, and S is a known constant matrix. This means that no matter what parameter vector is chosen to minimize J , it must simultaneously satisfy the set of constraints $\mathbf{c} = S\boldsymbol{\theta}$. Hence, there are less degrees of freedom available to minimize J . The solution to the problem

$$\hat{\boldsymbol{\theta}}_{\text{CLS}} = \underset{\boldsymbol{\theta} : \mathbf{c} = S\boldsymbol{\theta}}{\text{arg min}} J(Z, Z_{\mathcal{M}_1}) \quad (16)$$

is given by (Draper and Smith, 1998)

$$\hat{\boldsymbol{\theta}}_{\text{CLS}} = (\Psi^T \Psi)^{-1} \Psi^T \mathbf{y} - (\Psi^T \Psi)^{-1} S^T [S (\Psi^T \Psi)^{-1} S^T]^{-1} (S \hat{\boldsymbol{\theta}}_{\text{LS}} - \mathbf{c}). \quad (17)$$

As it will be shown in future sections, the solution (17) turns out to be very helpful when we are able to translate auxiliary information about the system \mathcal{S} in terms of a set of equality constraints on the parameters. Of course, this is easier to do for some model classes and hence this serves as motivation for choosing certain model classes depending on the available auxiliary information and our ability to code it in terms of constraints.

The issue of parameter estimation – or model training as known in other fields – is vast. A key-point which has not been dealt with because it would require a far more technical discussion has to do with the statistical properties of the noise \mathbf{e} in (12). Here it has been implicitly assumed that it is white. Whenever the noise is correlated, the LS estimator becomes biased. There are several solutions to this problem, for instance: i) if one can find a set of variables, called instruments, that are not correlated to the noise and remain correlated to the output, the *instrumental variable* estimator can be used (Young, 1970), ii) the model class can be changed to try to model

the correlation in the noise. A common choice is to add a *moving average* (MA) part to the model. The resulting model class is no longer linear-in-the-parameters and iterative estimators are available such as the *extended least squares* (Chen and Billings, 1989; Lu et al., 2001), and iii) by solving the problem in (11) (Aguirre et al., 2010).

The basic theory and algorithms can be found in most text-books some of which will be mentioned in Sec. 9. There are many alternative procedures for polynomial models such as (Nepomuceno et al., 2007; Wei and Billings, 2009) and also for other representations such as rational (Wu et al., 2008; Zhu and Billings, 1993), neural networks (Chen et al., 1990b; Masri et al., 1993) and radial basis functions (Chen et al., 1990a).

We close mentioning that although technical aspects of the estimators certainly depend on the model class used, many discussions in this section, especially those in Sec. 5.1 remain valid for other model classes (Ribeiro and Aguirre, 2018).

5.3 The danger of overparametrization

From what has been discussed in this section it is now possible to have a better understanding of the danger of overparametrizing a model. Let us consider problem (10) again. Would it be possible to find $\hat{\theta}$ such that $J(Z, Z_{\mathcal{M}_1}) = 0$? It might sound absurd (and in practice it is, in fact), but we can force $\hat{y}_1(k) = y(k)$, $\forall k$ for the estimation data. Hence, let us see under which conditions $\xi = 0$ in (13). For this, let's go back one step and consider (12). If we increase the size of θ to the point that $n_\theta = N$, then $\Psi \in \mathbb{R}^{N \times N}$ becomes a square matrix. Assuming that it is nonsingular, then $\hat{\theta} = \Psi^{-1}y$ and therefore $\xi = 0$. What we have done is to increase the number of degrees of freedom (parameters to be estimated) to match the number of “constraints” (the number of rows of Ψ) to end up with a square system of equations that has a single solution. Is that solution any good? Most likely not. And the reason is that all the uncertainties and noise in the data $y(k)$ will be fit by the model, which ideally should only fit the underlying dynamics of the system. The resulting model in this hypothetical case has a lot more parameters than needed – remember that $n_\theta = N$ – and therefore the model is said to be overparametrized.

An interesting remark on which we will not dwell here is this: if we consider problem (11) instead, we will not face the same problem. The reason is that in order to have $J(Z, Z_{\mathcal{M}_s}) = 0$ we would need to have $\hat{y}_s(k) = y(k)$, $\forall k$.

This will not be achieved in practice because $\hat{y}_s(k)$ is obtained by iterating the model (see Sec. 5.1) and an overparametrized model will, more often than not, be unstable, hence $\hat{y}_s(k) \neq y(k)$. This discussion then has two messages. First, problem (11) is definitely more robust than problem (10). Second, if the latter problem is the one being solved, then overparametrization is a real danger especially for NARMAX polynomial models and similar model classes.

6 Model Validation

We finally get to the last step in system identification. Here we would like to answer the question, does the model $\mathcal{M}(\hat{\theta})$ represent the underlying dynamics of the system?

One of the basic rules in model validation is to use a set of data Z_v for this purpose which is different from the data used to fit the model, that is the estimation or validation data Z . This is necessary because we cannot compare the model directly to the system \mathcal{S} as mentioned before. Then, in order to compare entities that are alike we take data from the system and data from the model $Z_{\mathcal{M}}$ and compare both using some kind of metric $V(Z_v, Z_{\mathcal{M}})$. It should come as no surprise that the choice of Z_v , $Z_{\mathcal{M}}$ and V have their influence on the validation. If there is only one set of data Z^N , then this should be divided into a part for identification Z^{N_i} and a part for validation $Z_v^{N_v}$, such that $N = N_i + N_v$. A common choice is to split the data such that $N_i = 2N_v$, but this is not a must.

As for Z_v , it is recommended that these data be measured from the system operating over a range (amplitude and frequency-wise) consistent with the intended use of the model. In obtaining the identification data Z it is reasonable to try to excite the system over the widest possible operating range (in the nonlinear case) in order to gather as much information as possible. When it comes to validation, there is no reason why we should request that the model be a faithful representation of the system over operating ranges that will not be visited in practice.

Concerning the choice of $Z_{\mathcal{M}}$, as discussed in Sec. 5.1, the use of $Z_{\mathcal{M}_s}$ should be strongly preferred over $Z_{\mathcal{M}_1}$. As a matter of fact, the latter is close to useless for model validation, because even poor models can produce OSA predictions that are close to the validation data. On the other hand, the use of $Z_{\mathcal{M}_s}$ is very exacting, and that is what is required in validation.

Finally, the use of a chosen metric V should be considered with care. Suppose that V is a measure of distance between two data sets. Also, consider two models with $Z_{\mathcal{M}_{s1}}$ and $Z_{\mathcal{M}_{s2}}$ such that $V(Z_v, Z_{\mathcal{M}_{s1}}) < V(Z_v, Z_{\mathcal{M}_{s2}})$. This only means that the first model is better than the second *with respect to the chosen metric V* . A certain metric might not be sufficiently specific to capture the dynamical aspects of the models. Common metrics are the mean squared error or the mean absolute percentage error, but the list is much longer.

Before mentioning some specific criteria, let it be said that the question: “is this model valid?” should be preceded by the question: “what is the intended use for the model?” In other words, the validity of a model should not be tackled as an absolute attribute, but rather as something that should make sense within a context. That is perhaps one of the greatest difficulties in model validation because very often we do not know exactly what to ask from the model.

6.1 Residual tests

This consist of testing the residual vector ξ for whiteness and for correlations with the input and output (Billings and Tao, 1991; Billings and Zhu, 1994). The main idea behind this procedure is that if the model structure is sufficiently flexible and the estimation procedure was sound, then all the correlations in the data should be explained by the model, hence the residuals should not be self-correlated and uncorrelated with the input and output. Also, because the standard linear correlation functions are unable to detect all nonlinear correlations, then specific nonlinear correlation functions should be used (Billings and Zhu, 1995; Zhu et al., 2007).

Because the residuals are defined based on the OSA prediction, clearly a model that passes the residual tests might still be inadequate from a *dynamical* point of view. Also, residual tests are not sensitive to overparametrization. That is, overparametrized models often pass residual tests.

6.2 Dynamical invariants

A rather particular situation arises when the system \mathcal{S} is chaotic. In that case it is quite common to use a number of dynamical and geometrical invariants to quantify the dynamics. Among such indices one can mention correlation dimension, Lyapunov exponents, Poincaré sections and bifurcation diagrams.

Some of these tools have been discussed in the context of model validation in (Haynes and Billings, 1994; Aguirre and Billings, 1994).

A more exacting procedure for model validation, but now restricted to 3D chaotic models is topological analysis (Letellier et al., 1995, 1996, 2002). This procedure builds topological templates from the system and model data and compares them. From such templates it is possible to extract the population of periodic orbits and to compare the model population to that of the original system. This is far more detailed, intricate and complicated than to just compare the appearance of attractors.

6.3 Synchronization

A very interesting procedure suggested in (Brown et al., 1994) is that of synchronization. The idea is that that underlies the concept of a state observer. An error signal between model output and data is fed back to the model to force the model output to follow the data. From the days of Huygens it is known that two coupled oscillators will synchronize if their natural frequencies (their intrinsic dynamics) be close. The same applies here. We would like to know if the model dynamics is close to the dynamics underlying the data. Hence we couple model and data and see if the “synchronization error” becomes small.

This procedure has two practical problems. First, in many cases synchronization can be achieved at the expense of increasing the coupling force. It has been pointed out that different dynamics can be made to synchronize and therefore synchronization has little to offer when it comes to (absolute) model validation (Aguirre et al., 2006; Letellier et al., 2018). Second, if the model does synchronize with large coupling, does this imply that the underlying dynamics have been learned by the model? The answer to this question is negative. However, if the model and data have the same dynamics, the coupling required for synchronization can be very small.

A practical approach to a similar problem has been put forward in (Aguirre et al., 2006). There the main goal is not to validate in absolute terms a model, but rather compare models and choose the one that is closest to the dynamics underlying the data. This was referred to as *model evaluation* in the aforementioned reference. To achieve this a measure of synchronization effort must be taken into account for the comparison to make any reasonable sense. Then if the maximum synchronization error is very different, it can be used to rank the models: the best model has the smallest maximum error.

However, often models have similar errors, in that case the synchronization effort is used. Hence given two models with similar errors, the one that required a smaller effort is the better model. So, in short synchronization allied to a measure of cost can help in comparing models, but not to get any general assessment of model quality.

7 Grey-Box Techniques

So far we have described system identification problems from a black-box point of view, that is, the only source of information about the system \mathcal{S} is the data set Z . Even if we assume that, say, the model order (n_y) and degree of nonlinearity (ℓ) are known, still we refer to this as black-box identification.

Now we move on to grey-box system identification problems where it is assumed that some additional information is available, which we will represent by \mathcal{I} as in Figure 4. This raises a number of interesting questions, such as:

1. what kind of auxiliary information \mathcal{I} is useful?
2. how does \mathcal{I} relate to the model class \mathcal{M}^c ?
3. assuming that \mathcal{I} and $\mathcal{M} \in \mathcal{M}^c$ are compatible, how do we actually use \mathcal{I} in determining $\mathcal{M}(\hat{\theta})$?

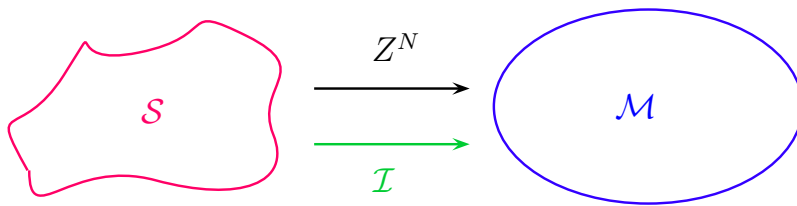


Figure 4: Simplified schematic diagram for grey-box identification, where \mathcal{S} represents the system that should be approximated by a model \mathcal{M} which is built from a set of measured data Z^N of length N and auxiliary information \mathcal{I} .

In what follows a glimpse to some grey-box techniques will be presented, and literature will be provided for details.

7.1 \mathcal{I} is the static function

We now assume that \mathcal{I} is the static function (calibration curve) of the system. To see this we must first consider the steady-state analysis of a NARX model.

Consider the NARX and deterministic part of model (3) taken in steady-state, that is, $\bar{y} = y(k-i)$, $\forall i$ and $\bar{u} = u(k-j)$, $\forall j$, then we have an *algebraic* polynomial of the form

$$\bar{y} = F_{\text{ss}}^{\ell}[\bar{y}, \bar{u}]. \quad (18)$$

It is left to the reader to verify that the parameters of the right-hand-side of (18) are the cluster coefficients (Aguirre and Billings, 1995b; Aguirre et al., 2002). Equation (18) says that if a constant input \bar{u} is applied to the NARX dynamical model, then in steady-state, if the model is asymptotically stable, the output $y(k)$ will settle to \bar{y} . This is very closely related to the concept of fixed-points of autonomous models and the number of such equilibria is *given by the highest power of the output*, for which ℓ is an upper bound (Aguirre and Mendes, 1996). For example, model

$$y(k) = \theta_1 y(k-1) + \theta_2 y(k-1)^3 + \theta_3 u(k-2)y(k-1)$$

has three fixed points for each constant value of the input, whereas the model

$$y(k) = \theta_1 y(k-1) + \theta_2 y(k-1)^2 u(k-1) + \theta_3 u(k-2)y(k-1),$$

for which $\ell = 3$ – as for the previous one – only has two fixed points for each constant value of the input.

In cases for which there is a “calibration curve” for the system this will correspond to F_{ss}^{ℓ} in (18) and no output regressors of degree 2 or higher are needed to reproduce the calibration curve, as seen in the next example.

Example 1. This example uses data measured from a small thermal pilot plant (Aguirre et al., 2002). Because there is no multi-stability, that is, for a given input in steady-state \bar{u} there will be only *one* value for the output \bar{y} , it is possible to remove all potential regressors from clusters Ω_{y^p} , $p > 1$. That is, quadratic and cubic regressors in y need not be considered, nor crossed terms $\Omega_{y^p u^m}$, $p > 1$, $\forall m$. Besides, because the static data look quadratic (see Fig.5), the cluster Ω_{u^3} was also removed from the set of candidate regressors. This set of actions is already due to what we find in \mathcal{I} .

The following black-box model was then obtained:

$$\begin{aligned}
y(k) = & 1.2929y(k-1) + 0.0101u(k-2)u(k-1) + 0.0407u(k-1)^2 \\
& -0.3779y(k-2) - 0.1280u(k-2)y(k-1) \\
& +0.0957u(k-2)y(k-2) + 0.0051u(k-2)^2.
\end{aligned} \tag{19}$$

In steady state, model (19) can be written thus

$$\begin{aligned}
\bar{y} = & 1.2929\bar{y} + 0.0101\bar{u}^2 + 0.0407\bar{u}^2 - 0.3779\bar{y} - 0.1280\bar{u}\bar{y} \\
& +0.0957\bar{u}\bar{y} + 0.0051\bar{u}^2,
\end{aligned} \tag{20}$$

which has a static nonlinearity of the form

$$\bar{y} = \frac{\Sigma_{u^2}\bar{u}^2}{1 - \Sigma_y - \Sigma_{yu}\bar{u}}. \tag{21}$$

In a typical grey-box problem, we want to estimate the cluster coefficients Σ_{u^2} Σ_{yu} Σ_y in such a way that (21) fits the measured static data Fig. 5. Because, (21) is not linear-in-the-parameters, then such a fit must be accomplished by some nonconvex optimization algorithm. Here a quasi-Newton FBS method was used to find: $\mathbf{c} = [\Sigma_{u^2} \Sigma_{yu} \Sigma_y]^T = [0,0615 \ -0,0360 \ 0,9128]^T$. This can then be written in terms of a set of three linear constraints

$$\begin{aligned}
\begin{bmatrix} 0,0615 \\ -0,0360 \\ 0,9128 \end{bmatrix} &= \begin{bmatrix} 0 & 1 & 1 & 0 & 0 & 0 & 1 \\ 0 & 0 & 0 & 0 & 1 & 1 & 0 \\ 1 & 0 & 0 & 1 & 0 & 0 & 0 \end{bmatrix} \begin{bmatrix} \theta_1 \\ \theta_2 \\ \theta_3 \\ \theta_4 \\ \theta_5 \\ \theta_6 \\ \theta_7 \end{bmatrix}. \tag{22} \\
\mathbf{c} &= S\boldsymbol{\theta}.
\end{aligned}$$

Notice that θ_2 , θ_3 and θ_7 are the only parameters of the term cluster Ω_{u^2} (quadratic input terms), hence their addition is Σ_{u^2} by definition. That composes the first constraint in (22) and so on.

The set of constraints in (22) and the parameter vector $\hat{\boldsymbol{\theta}}_{\text{LS}}$ of the model in (19) – which was obtained by unconstrained estimation – can be used with

the constrained estimator (17) to yield the model (notice that the model structure is the same):

$$\begin{aligned}
 y(k) = & 1.2796y(k-1) + 0.0178u(k-2)u(k-1) + 0.0408u(k-1)^2 \\
 & -0.3668y(k-2) - 0.2565u(k-2)y(k-1) \\
 & +0.2205u(k-2)y(k-2) + 0.0029u(k-2)^2,
 \end{aligned} \tag{23}$$

which *by construction* has the desired static function.

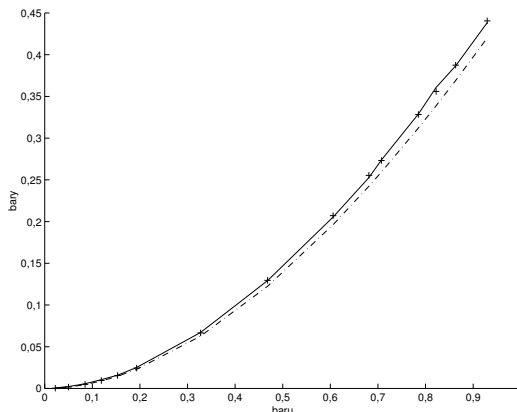


Figure 5: Static functions of identified models (—) measured; (---) unconstrained model (19) and (×) constrained model (23).

As will be illustrated below in Example 2, there is a simpler way to proceed which will not require a non convex optimization step. The price paid will be that the full static function will not be imposed, but rather only some user-chosen steady-state data points.

In closing, it is interesting to point out that \mathcal{I} can be used either way. Here, we assume that \mathcal{I} is known beforehand and we use such info in building the model. Moving in the other direction, it is possible to, from an estimated model, to extract, say, the static function (Aguirre, 1997; Aguirre et al., 2002). This last procedure proves to be very handy in estimating Hammerstein and Wiener models from identified NARX models (Aguirre et al., 2005b).

7.2 \mathcal{I} is steady-state data

The next case that will be considered is when the auxiliary information \mathcal{I} is a set of steady-state data $\bar{\mathbf{u}} = [\bar{u}_1, \dots, \bar{u}_M]^T$ and the corresponding output

values $\bar{\mathbf{y}} = [\bar{y}_1, \dots, \bar{y}_M]^T$. Let us indicate the steady-state data as $\mathcal{I} = Z_{\text{ss}}^M = [\bar{\mathbf{u}}, \bar{\mathbf{y}}]$. Of course, we still assume that there is the set of dynamical data $Z^N = [u(k), y(k)]$, $k = 1, 2, \dots, N$. A loose grey-box problem would be: given Z^N and Z_{ss}^M , find a model $\mathcal{M}(\hat{\boldsymbol{\theta}})$ that *simultaneously* uses both data sets. In what follows this aim will be made more precise.

If the dynamics of the system \mathcal{S} do not change significantly over a certain range of operating conditions, but only the gain, that is, the static function is nonlinear, then the procedure to be described in what follows is a workable solution to not having to perform large-amplitude dynamical tests on the system. The dynamical data Z^N can be collected over a rather narrow operating range and the information of the system static nonlinearity *far* from such a range comes in through Z_{ss}^M .

7.2.1 Constraining parameters

One way of using $\mathcal{I} = Z_{\text{ss}}^M = [\bar{\mathbf{u}}, \bar{\mathbf{y}}]$ in addition to Z^N is to use \mathcal{I} to derive parameter constraints and then use such result with (17). This was already done in Example 1, but there the set of constraints was built from a nonlinear fit of an algebraic relation (21) to the static data. Here we want to avoid solving a nonconvex optimization problem and to take the constraints directly from the data. To see how to do this, notice that in the case of NARX polynomials the steady-state relation (18) will yield a linear constraint for each steady-state point in $Z_{\text{ss}}^M = [\bar{\mathbf{u}}, \bar{\mathbf{y}}]$. Such a constraint can be then used in (17) which also uses Z^N . It should be noticed that not all model classes will yield linear constraints. Therefore there *is* a connection between the model class and \mathcal{I} . This will be seen in the following example.

Example 2. Let us start with a simple hypothetical example. Let us assume that the model structure is given by

$$\begin{aligned} y(k) = & \theta_1 y(k-1) + \theta_2 y(k-2) + \theta_3 u(k-1) + \theta_4 u(k-2)^2 \\ & + \theta_5 u(k-1)u(k-2) + \theta_6 u(k-2). \end{aligned} \quad (24)$$

It is further assumed that we have dynamical and static data Z and Z_{ss} . To estimate the unknown parameters θ_i , $i = 1, \dots, 6$ from Z is well-known problem. For instance, using the classical Least Squares estimator (14) the parameter vector $\hat{\boldsymbol{\theta}}_{\text{LS}}$ is readily obtained. Now suppose that apart from using Z we want to make sure that the static function of (24) passes through two

of the points in Z_{ss} , say $[\bar{u}_3, \bar{y}_3]$ and $[\bar{u}_7, \bar{y}_7]$. We start by writing model (24) in steady-state thus:

$$\bar{y} = (\theta_1 + \theta_2)\bar{y} + (\theta_3 + \theta_6)\bar{u} + (\theta_4 + \theta_5)\bar{u}^2.$$

Hence the two constraints are

$$\begin{aligned}\bar{y}_3 &= (\theta_1 + \theta_2)\bar{y}_3 + (\theta_3 + \theta_6)\bar{u}_3 + (\theta_4 + \theta_5)\bar{u}_3^2 \\ \bar{y}_7 &= (\theta_1 + \theta_2)\bar{y}_7 + (\theta_3 + \theta_6)\bar{u}_7 + (\theta_4 + \theta_5)\bar{u}_7^2,\end{aligned}$$

which can be rewritten as $\mathbf{c} = S\boldsymbol{\theta}$ with

$$\mathbf{c} = \begin{bmatrix} \bar{y}_3 \\ \bar{y}_7 \end{bmatrix}; \quad S = \begin{bmatrix} \bar{y}_3 & \bar{y}_3 & \bar{u}_3 & \bar{u}_3^2 & \bar{u}_3^2 & \bar{u}_3 \\ \bar{y}_7 & \bar{y}_7 & \bar{u}_7 & \bar{u}_7^2 & \bar{u}_7^2 & \bar{u}_7 \end{bmatrix}. \quad (25)$$

Now, as in Example 1, with \mathbf{c} , S and $\hat{\boldsymbol{\theta}}_{\text{LS}}$, the constrained estimator (17) can be used to find another parameter vector $\hat{\boldsymbol{\theta}}_{\text{CLS}}$ which *exactly* satisfies the two aforementioned constraints and *approximately* – in a least squares sense – fits the dynamical data Z .

7.2.2 Imposing a transcritical bifurcation

The reason for inserting an example on the imposition of a fixed-point bifurcation here demands a short explanation that can be announced in two steps. First, the normal equations of fixed-point bifurcations for maps are (first-order) difference equations. Second, bifurcations relate to steady-state behavior of dynamical systems. Therefore the conditions for the occurrence of certain bifurcations can be found from first-order autoregressive equations. In a sense, a bifurcation diagram can be seen as a particular case of a steady-state function of a nonlinear polynomial model if the input is used as “bifurcation parameter”. The following example illustrates the case for a transcritical bifurcation which has the appearance of a static function with dead-zone. Other examples include period-doubling bifurcation (Aguirre and Furtado, 2007) and the Hopf (Neimark-Sacker) bifurcation (Aguirre and Rodrigues, 2012).

Example 3. For details on this example see (Aguirre, 2014). Consider a Hammerstein system with static function given by:

$$z(k) = \begin{cases} 0, & \text{if } u(k) < 1 \\ u(k) - 1, & \text{if } u(k) \geq 1, \end{cases}$$

with linear dynamics described by:

$$y(k) = 0.9y(k-1) + 0.7z(k-1) + e(k), \quad (26)$$

where the input is $u(k) \sim U(1, 0.6)$, that is a uniform random signal with mean equal to one and standard deviation $\sigma = 0.6$. The output was simulated using (26) with $e(k) \sim \text{WGN}(0, 0.1)$ which is a zero mean white Gaussian noise with standard deviation $\sigma = 0.1$. The data $Z = [u(k) \ y(k)]$, $k = 101, \dots, 300$ were used to estimate three models. The model structure was automatically determined using the ERR criterion (5). The models were tested on the validation data $Z_v = [u(k) \ y(k)]$, $k = 301, \dots, 500$.

The black-box model \mathcal{M}_1 was:

$$\begin{aligned} y(k) = & +0.8676 y(k-1) + 0.37369 u(k-1)^2 - 0.36828 u(k-1) \\ & +0.09723 + 0.86609 \times 10^{-2} u(k-3)^2, \end{aligned} \quad (27)$$

for which the static behaviour is shown in Figure 6 which is clearly rather poor. This would be expected because, being a NARX polynomial (27) also has a polynomial and therefore smooth static function, as indicated in Figure 6 by the blue tracing.

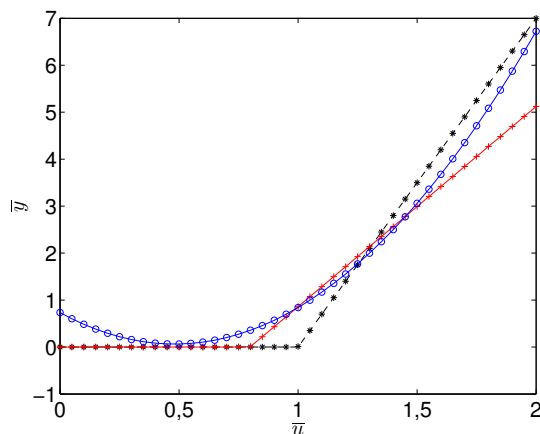


Figure 6: Black dashed is the original nonlinear static function; blue circles indicate the static function of black-box model \mathcal{M}_1 (27); the red crosses correspond to grey-box model \mathcal{M}_2 (29) and the asterisks, to another grey-box model \mathcal{M}_3 (32).

We move a step forward and assume that the static function is formed by two line segments. In order to make this more understandable, the following result is quoted from (Aguirre, 2014):

Lemma 1 *A NARX polynomial model with $\ell \geq 2$ for which the only nonzero cluster coefficients are Σ_y , Σ_{uy} and Σ_{y^2} has the following two sets of equilibria:*

$$\bar{Y}_1 = \bar{y} = 0 \quad \text{and} \quad \bar{Y}_2(\bar{u}) = \bar{y} = \frac{1 - \Sigma_y}{\Sigma_{y^2}} - \frac{\Sigma_{uy}}{\Sigma_{y^2}} \bar{u},$$

which intercept at

$$\bar{u}_c = \frac{1 - \Sigma_y}{\Sigma_{uy}}. \quad (28)$$

If, in addition, the sets of equilibria \bar{Y}_1 and \bar{Y}_2 exchange stability at \bar{u}_c we have a *transcritical bifurcation*.

The information in Lemma 1 can be used – see (Aguirre, 2014) for details – to obtain a model \mathcal{M}_2 by removing Ω_u and the constant term from the set of candidates:

$$\begin{aligned} y(k) = & +0.80721 y(k-1) + 0.24200 u(k-1)^2 \\ & -0.10572 u(k-3)u(k-1) + 0.02141 u(k-3)y(k-1) \\ & +0.03838 u(k-3)^2 + 0.63554 \times 10^{-2} y(k-1)^2, \end{aligned} \quad (29)$$

which is also unable to fit the static function of the system, although the auxiliary information that the static function is composed of two line segments (these are the two sets of equilibria mentioned in Lemma 1) was correctly implemented, as seen in Figure 6.

We now use the information in Lemma 1 which relates to the location of the break point at $\bar{u}_c = 1$ and the inclination $\alpha = 7$ of the second part of the static function ($\bar{Y}_2(\bar{u})$ in the lemma). Hence the following constraints can be written

$$0 = \Sigma_{u^2}, \quad 1 = \frac{1 - \Sigma_y}{\Sigma_{uy}}, \quad 7 = -\frac{\Sigma_{uy}}{\Sigma_{y^2}}. \quad (30)$$

The second, third and fifth parameters of (29) compose Σ_{u^2} . Therefore the summation of the three of them must be zero. This is the first constraint. The other two are built in a similar way. Hence the set of constraints is in the form $\mathbf{c} = S\boldsymbol{\theta}$ with

$$\mathbf{c} = \begin{bmatrix} 0 \\ 1 \\ 0 \end{bmatrix}; \quad S = \begin{bmatrix} 0 & 1 & 1 & 0 & 1 & 0 \\ 1 & 0 & 0 & 1 & 0 & 0 \\ 0 & 0 & 0 & 1 & 0 & 7 \end{bmatrix}. \quad (31)$$

Finally, model \mathcal{M}_3 was estimated using (17)

$$\begin{aligned} y(k) = & +0.82469 y(k-1) + 0.25589 u(k-1)^2 \\ & -0.15788 u(k-3)u(k-1) + 0.17531 u(k-3)y(k-1) \\ & -0.09801 u(k-3)^2 - 0.02505 y(k-1)^2, \end{aligned} \quad (32)$$

which is able to reproduce the dead-zone type of static function (see Figure 6). Once the auxiliary information \mathcal{I} is described in terms of constraints (30), the constrained least squares estimator (17) can be readily used. The trick then is to be able to translate \mathcal{I} into constraints that, of course, will depend on the model class being used. The details of that development for this and similar examples can be found in (Aguirre, 2014).

It is noted that the root mean square error on the dynamical data is 0.222 for \mathcal{M}_1 , 0.350 for \mathcal{M}_2 and 0.316 for \mathcal{M}_3 . This shows a fact which is that often the unconstrained model will perform better on dynamical data but far worse on static data. Hence, when dynamical and static performances are conflicting objectives (more on this later), it is possible to give up a bit of dynamical performance to improve the model steady-state, as for \mathcal{M}_3 in this example.

7.2.3 Biobjective parameter estimation

In the previous section the auxiliary information \mathcal{I} was coded in terms of equality constraints. Hence such hard constraints were the means by which \mathcal{I} found its way into the model. In this section a different approach will be described.

For the sake of presentation, only the biobjective case will be described, although more objectives can be taken into account (Nepomuceno et al., 2007).

In biobjective optimization we do not search for a *single optimal* solution that simultaneously minimizes two cost functions. Instead the aim is to find a set Θ^* of solutions θ^* called the Pareto set (Chankong and Haimes, 1983)

$$\theta^* \in \Theta^* \Leftrightarrow \{\nexists \theta : \mathbf{J}(\theta) \leq \mathbf{J}(\theta^*) \text{ and } \mathbf{J}(\theta) \neq \mathbf{J}(\theta^*)\}, \quad (33)$$

where $\mathbf{J}(\theta)$ is a vector of cost functions. In (33) the symbol “ \leq ” indicates that all elements of a vector are less or equal to the corresponding elements of the other vector. An often-used choice is:

$$\mathbf{J}(\theta) = [J(Z, Z_{\mathcal{M}_1}) \quad J(Z_{ss}, Z_{\mathcal{M}_{ss}})]^T, \quad (34)$$

where $Z_{\mathcal{M}_{\text{ss}}}$ is the data produced by model \mathcal{M} taken in steady-state. The solutions $\boldsymbol{\theta}^*$ can be found solving (Nepomuceno et al., 2004, 2007)

$$\hat{\boldsymbol{\theta}}_{\text{BO}} = \arg \min_{\boldsymbol{\theta} \in \mathbf{D}} \lambda J(Z, Z_{\mathcal{M}_1}) + (1 - \lambda) J(Z_{\text{ss}}, Z_{\mathcal{M}_{\text{ss}}}), \quad (35)$$

where $0 \leq \lambda \leq 1$ and \mathbf{D} is the set of viable solutions. For each value of λ one estimates $\boldsymbol{\theta}^*(\lambda)$, which is part of the Pareto set. The mono-objective solutions that minimize $J(Z, Z_{\mathcal{M}_1})$ and $J(Z_{\text{ss}}, Z_{\mathcal{M}_{\text{ss}}})$ are obtained from (35) $\lambda = 0$ and $\lambda = 1$, respectively. An interesting interpretation of (35) is that it is the Least Squares estimator with a regularization term taken from the static data, which is the available auxiliary information in this case.

In order to provide some details on how this can be achieved, the following results are required:

Definition 1 *Affine Information (Nepomuceno et al., 2007). Consider the parameter vector $\boldsymbol{\theta} \in \mathbb{R}^{n_\theta}$, a vector $\mathbf{v} \in \mathbb{R}^p$ and a matrix $G \in \mathbb{R}^{p \times n_\theta}$. Both \mathbf{v} and G are assumed to be accessible. Moreover, suppose $G\boldsymbol{\theta}$ constitutes an estimate of \mathbf{v} , such that $\mathbf{v} = G\boldsymbol{\theta} + \epsilon$, where $\epsilon \in \mathbb{R}^p$ is an error vector. Then $[\mathbf{v}, G]$ is said to be an affine information pair of the system.*

Theorem 1 *(Nepomuceno et al., 2007) Let $[\mathbf{v}_i, G_i]$ with $i = 1, \dots, m$ be m affine information pairs related to a system, where $\mathbf{v}_i \in \mathbb{R}^{p_i}$ and $G_i \in \mathbb{R}^{p_i \times n_\theta}$. Assume that at least one of the matrices G_i is full column rank. Let \mathcal{M} be a given model structure which is linear in the parameter vector $\boldsymbol{\theta} \in \mathbb{R}^{n_\theta}$. Then the m affine information pairs can be simultaneously taken into account while estimating the parameters of model \mathcal{M} , by solving*

$$\hat{\boldsymbol{\theta}}_{\text{MO}} = \arg \min_{\boldsymbol{\theta}} \sum_{i=1}^m w_i (\mathbf{v}_i - G_i \boldsymbol{\theta})^\top (\mathbf{v}_i - G_i \boldsymbol{\theta}), \quad (36)$$

with $\mathbf{w} = [w_1 \ \dots \ w_m]^\top \in W$. The unique solution of (36) is given by

$$\hat{\boldsymbol{\theta}}_{\text{MO}} = \left[\sum_{i=1}^m w_i G_i^\top G_i \right]^{-1} \left[\sum_{i=1}^m w_i G_i^\top \mathbf{v}_i \right]. \quad (37)$$

In (35) the multiobjective problem has been reduced to a biobjective one ($m = 2$) with $w_1 = \lambda$ and $w_2 = 1 - \lambda$, $G_1 = \Psi$ is the matrix of “dynamical”

regressors and G_2 would be composed of regressors taken in steady-state. Also, $\mathbf{v}_1 = \mathbf{y}$ and $\mathbf{v}_2 = \bar{\mathbf{y}}$.

Once the Pareto set is obtained, varying λ in the range $0 \leq \lambda \leq 1$, it is often desirable to pick one model, one way of doing this was proposed by Barroso et al. (2007). Each candidate model $\boldsymbol{\theta}$ in the Pareto set Θ^* is simulated in free-run mode and the output is indicates as:

$$\hat{y}(k) = \hat{\boldsymbol{\psi}}^T(k-1)\boldsymbol{\theta}, \quad (38)$$

where the hat in $\hat{\boldsymbol{\psi}}(k-1)$ indicates that previously simulated values are used. The corresponding error is:

$$\eta(k) = y(k) - \hat{y}(k). \quad (39)$$

Now, define

$$J_{\text{corr}}(\boldsymbol{\theta}) = \left| \frac{1}{N} \sum_{k=1}^N \eta(k)\hat{y}(k) \right|. \quad (40)$$

Barroso has argued that $J_{\text{corr}}(\boldsymbol{\theta})$ will achieve its lowest value for the best $\boldsymbol{\theta}$ (Barroso et al., 2007).

An interesting remark concerning multiobjective estimation in grey-box system identification is that it provides a mechanism by which auxiliary information \mathcal{I} can be taken into account. Not in the form of constraints, but rather by defining a cost function for which smaller values correspond to models that better incorporate \mathcal{I} . Since one of the objectives will still be to fit the dynamical data, then various types of auxiliary information can be used to compose a multiobjective optimization problem. In this section bi-objective optimization was used in the context of parameter estimation. Hafiz has investigated approaches in the context of both, structure selection and parameter estimation (Hafiz et al., 2020a,b).

7.3 Other types of auxiliary information

In what follows other types of auxiliary information \mathcal{I} that were used in the context of grey-box identification will be listed.

One of the basic forms of \mathcal{I} is that of the shape of the static function. The use of such information has been used in (Aguirre, 1997; Aguirre et al., 2000). Another basic form of \mathcal{I} is the location of fixed-points. As a matter of fact, as discussed in this work, the static curve of a system can be interpreted as

a *continuum* of fixed points as a function of the input. Relationships of how the number, location and symmetry of fixed points relate to the structure of polynomial models have been presented in (Aguirre and Mendes, 1996).

A key point in this way of using \mathcal{I} is to establish relationships between model structure and types of information. Some results for polynomial NARX models were developed in (Aguirre and Jácome, 1998; Aguirre et al., 2002). Static functions were used for grey-box identification of rational models (Corrêa et al., 2002), polynomial models (Aguirre et al., 2004a) and radial basis models in (Aguirre et al., 2007).

Symmetry of the flow in state space was a key piece of information used to solve certain modelling problems via grey-box identification (Aguirre et al., 2004b, 2008a) and in the design of systems (Chen et al., 2008).

Because the normal forms of bifurcations in maps are polynomial, certain aspects of bifurcations of equilibria can be used in \mathcal{I} . In particular, the *flip*, or period-doubling bifurcation was used in (Aguirre and Furtado, 2007), Hopf (Neimark-Sacker) bifurcation was imposed on identified maps in (Aguirre and Rodrigues, 2012) and the transcritical bifurcation was used to reproduce non-smooth static functions in (Aguirre, 2014).

For systems that are known to display hysteresis, a specific choice of inputs can be used to guarantee multi-stability (Martins and Aguirre, 2016), which is a condition for hysteresis. More recently, an additional constraint was shown to be fundamental in order to guarantee that the system remains on the hysteresis loop in the case the input becomes constant (Abreu et al., 2020). In the first case study discussed in Section 8, a step further will be given: not only will the appearance of the hysteresis loop be guaranteed by the use of a specific class of inputs, but also, the shape of the loop will be modified by the use of parameter constraints.

A somewhat different approach has been followed in (Wu et al., 2020). In that work the authors use two sets of data of the same type, e.g. both coming from dynamical tests. However, the knowledge about the system conveyed by each data set is different. Then, one of the data sets is considered \mathcal{I} to the next.

The problem of using equality constraints on the states has been considered in (Ricco and Teixeira, 2021). In that paper, the problem has been solved in two steps: first the constraints are mapped from state variables to matrix parameters and then the problem is vectorized in order to apply standard algorithms. The region of attraction of the equilibrium point has been used as auxiliary information – called side information – in (Khosravi

and Smith, 2021).

8 Examples and Case Studies

The literature that has been cited so far provides many examples – simulated and experimental – of identification problems. Here three examples will be briefly presented for the sake of illustration with some emphasis on grey-box solutions.

8.1 Pneumatic valve with hysteresis

The data used in this example have been collected by Petrus Abreu, Lucas Tavares and Guilherme Mello from a laboratory pilot plant. Previous studies of the dynamics and steady-state features have been reported elsewhere (Aguirre, 2014; Ribeiro and Aguirre, 2018). Valves are widely used in industrial process control although they suffer from loss of performance due to nonlinearities and friction. For this reason the compensation of such effects has been investigated (Romano and Garcia, 2011; Baeza and Garcia, 2018; Abreu et al., 2020; Tavares et al., 2022).

The aim in this example is to illustrate results from (Martins and Aguirre, 2016) and Sec. 7.2 and to show how a hysteresis loop may be obtained using NARX polynomial models. In the sequel, it will be shown how the use of constraints can be employed to alter the format of the obtained loop.

The identification data are shown in Figure 7. The input and output are voltage signals, as indicated in the figure and explained in the caption. The units of such signals will be omitted henceforth. Such data were collected at a sampling frequency of 100 Hz and later decimated by a factor of 10. The identification data length was $N = 1700$.

Four models will be mentioned in what follows. We start with a very simple model which has three regressors: $y(k-1)$, $u(k-1)$ and the constant. Such a model presents a mean absolute percentage error of about $\text{MAPE} \approx 6\%$, but being an affine model it is not expected to reproduce anything that resembles hysteresis. In fact, following the discussion by Prof. Bernstein, this can be checked by exciting the model with a loading-unloading signal of decreasing frequency. As the input frequency diminishes any loops seen on the $u(k) - y(k)$ plane will collapse to a single curve (Bernstein, 2007). This

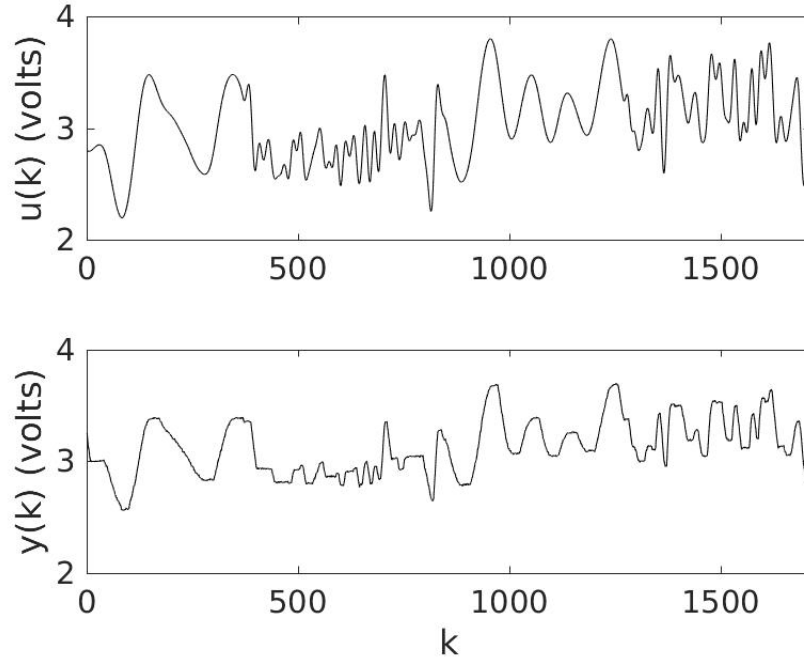


Figure 7: Input (top) output (bottom) data from a pneumatic valve. The input is a voltage signal sent to a V/I converter, and subsequently to an I/P converter which manipulates a pressure source. The output, also a voltage, is the movement of the actuator stem, collected by a position sensor.

is seen in the top of Figure 8 where the static function of this three-term model is just a line, as expected.

The second model considered is a thirteen-term nonlinear model with up to cubic nonlinear terms ($\ell = 3$) and maximum lags of two $n_u = n_y = 2$. Although this model presents a slightly better dynamical performance with $\text{MAPE} \approx 4.7\%$, it does not reproduce any hysteresis behavior. This is seen by noticing that as the frequency of the input forcing reduces, the model settles to a static function which is a slight curve as seen in the top of Figure 8. It has been pointed out that more often than not, models obtained in a black-box fashion do not present hysteresis (Martins and Aguirre, 2016). In what follows, certain modeling decisions – which clearly constitute grey-box procedures – will be made in order to guarantee that the identified models

will have hysteresis.

The third model considered in this example is shown below:

$$\begin{aligned}
 y(k) = & +0.80665 y(k-1) + 0.02888 u(k-1) + 0.30362 \\
 & +0.57737 u_2(k-1)u(k-1) - 0.52294 u_2(k-1)y(k-1) \\
 & +0.022105 u(k-1)y(k-1) - 0.00864 u_3(k-1)u(k-1) \\
 & +0.00787 u_3(k-1)y(k-1), \tag{41}
 \end{aligned}$$

where $u_2(k)$ is the first difference of the input signal, that is, $u_2(k) = u(k) - u(k-1)$ and $u_3(k) = \text{sign}[u_2(k)]$. The static behavior of model (41) is attained by assuming a constant input $\bar{u} = u(k)$, $\forall k$, and $u_2(k) = 0$. In addition to that, for loading periods $u_3(k) = 1$ and for unloading $u_3(k) = -1$. The use of regressors in $u_3(k)$ is recommended for hysteretic systems (Martins and

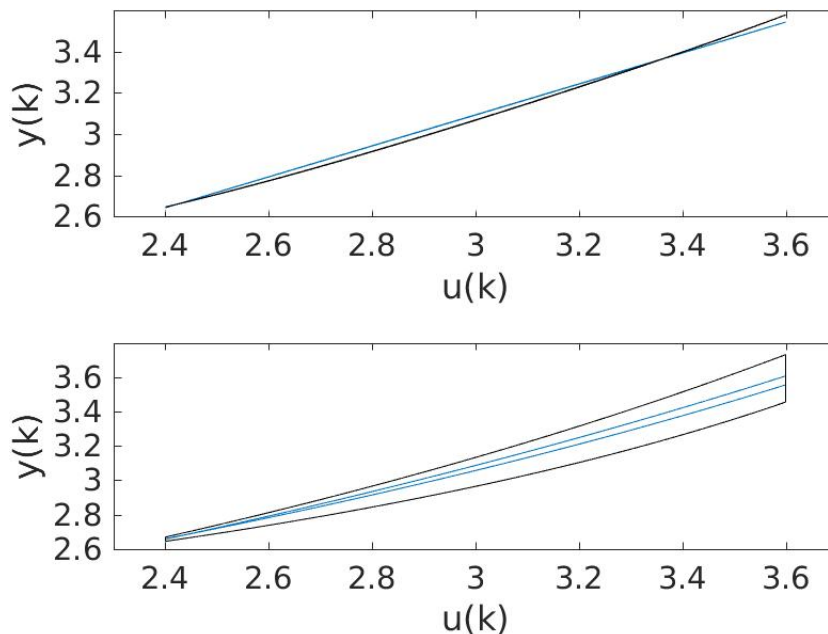


Figure 8: Top: static functions for three-term affine model (straight line in light blue) and thirteen-term nonlinear black-box model (slight curve in black). Bottom: static functions with hysteresis loops for model (41) (thin loop in light blue) and for a parameter-constrained model (wider hysteresis loop in black).

Aguirre, 2016). Hence the decision of including u_2 and especially u_3 was based on the auxiliary information \mathcal{I} that the system presents hysteresis. This, of course, constitutes a grey-box procedure. Although the dynamical behavior has not changed significantly (MAPE $\approx 5\%$), the novelty is that model (41) does have a hysteresis loop, as shown in the bottom part of Figure 8. In fact such a model has two equilibria, one for loading, given by

$$\bar{y} = \frac{(\theta_2 + \theta_7)\bar{u} + \theta_3}{1 - \theta_1 - \theta_8 - \theta_6\bar{u}} \quad (42)$$

and one for unloading:

$$\bar{y} = \frac{(\theta_2 - \theta_7)\bar{u} + \theta_3}{1 - \theta_1 + \theta_8 - \theta_6\bar{u}}, \quad (43)$$

where the θ 's are given in the same order as that of the parameters in model (41).

Now because we have valve data collected in steady-state, this is the auxiliary information \mathcal{I} in this problem, we would like to make sure that the identified model has a static function with a hysteresis loop that better resembles the static data. This can be achieved by building parameter constraints, as discussed in Sec. 7.2.1, from such data. In particular we write

$$\mathbf{c} = \begin{bmatrix} \bar{y}^1 \\ \bar{y}^2 \\ \bar{y}^3 \\ \bar{y}^4 \end{bmatrix}; \quad S = \begin{bmatrix} \bar{y}^1 & \bar{u}^1 & 1 & 0 & 0 & \bar{u}^1\bar{y}^1 & \bar{u}^1 & \bar{y}^1 \\ \bar{y}^2 & \bar{u}^2 & 1 & 0 & 0 & \bar{u}^2\bar{y}^2 & \bar{u}^2 & \bar{y}^2 \\ \bar{y}^3 & \bar{u}^3 & 1 & 0 & 0 & \bar{u}^3\bar{y}^3 & -\bar{u}^3 & -\bar{y}^3 \\ \bar{y}^4 & \bar{u}^4 & 1 & 0 & 0 & \bar{u}^4\bar{y}^4 & -\bar{u}^4 & -\bar{y}^4 \end{bmatrix}, \quad (44)$$

where the superscripts indicate a specific data point, that is, $(\bar{u}^1, \bar{y}^1) = (1.8, 2.112)$, $(\bar{u}^2, \bar{y}^2) = (3.4, 3.249)$, $(\bar{u}^3, \bar{y}^3) = (1.7, 2.211)$ and $(\bar{u}^4, \bar{y}^4) = (2.7, 2.843)$ are four desired points, the two first on the loading part of the hysteresis loop, and the other two on the unloading side. Then, using estimator (17) a new set of parameter values is attained and the hysteresis loop is wider, as seen in Figure 9 and has (MAPE $\approx 6\%$). The slight increase in the value of MAPE is somewhat expected because as we have imposed four steady-state constraints there are less degrees of freedom to fit the dynamical data.

As seen in the bottom part of Figure 8, the hysteresis loop of the constrained model is indeed wider than when the auxiliary information was not

used. Besides, the static function of the constrained model compares favorably to the collected data, as seen in Figure 9.

It has been verified that for some model-based control strategies applied to systems with hysteresis the use of auxiliary information was important. In particular, the control laws implemented from grey-box models clearly outperformed those based on black-box models (Abreu et al., 2020).

The aim of this example has been to illustrate the use of grey-box techniques in dealing with data measured from a system known to have hysteresis. The next two examples illustrate other aspects of grey-box techniques in other applications.

8.2 Dynamical and steady state data from an oil well

This case study has been developed in cooperation with colleagues in academia and industry (Aguirre et al., 2017).

“Downhole pressure is an important process variable in the operation of gas-lifted oil wells. The device installed in order to measure this variable is often called a Permanent Downhole Gauge (PDG). Replacing a faulty PDG

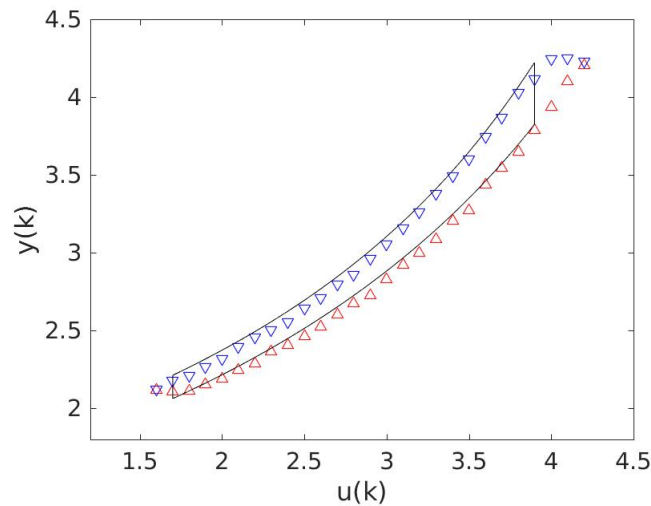


Figure 9: Static function with hysteresis loops for the constrained model (continuous lines) and valve data collected in steady-state for (red) \triangle increasing inputs, and (blue) ∇ decreasing inputs.

is often not economically viable and to have an alternative estimate of the downhole pressure is an important goal” (Aguirre et al., 2017). One way around this problem is to develop softsensors, that is, build models that will estimate the variable of interest (downhole pressure) from readily available measurements. Of course, this means that the models must be identified before the PDG becomes faulty. After the PDG becomes inoperative, a valid model can be used to provide an estimate for the said pressure. More details about this application can be found in (Teixeira et al., 2014; Aguirre et al., 2017).

This challenge was faced exclusively from historical data, that is, no specific testing was performed. If, on the one hand, this sounds an advantage, on the other, there is a cost to pay for that. In historical data most of the time the process is in steady state. Hence, in order to find windows of data that will bring forth the process dynamics, special care must be taken. The inspection of the database by an expert in the search for useful transients is both slow and tedious. In order to overcome this, an automatic procedure was developed and used (Ribeiro and Aguirre, 2015). The authors of (Pitino et al., 2020) have investigated the impact of the window of data on the performance of the identified model. They have put forward two procedures to select adequate windows of data in the context of linear thermal models.

Not everything is bad in historical data of this sort. There is a lot of steady state information. In fact, it is possible to attain high quality steady-state data by averaging over rather long windows of data. As discussed in Section 7 steady-state information can be used to great advantage in the identification of *dynamical* models, so long it is treated as auxiliary information \mathcal{I} which is additional to a set of dynamical data Z .

As an example of a SISO (single-input single-output) polynomial model, a six-term model was estimated using the following metaparameters: $\ell = 2$, $n_y = n_u = 3$ and $n_e = 1$, with downhole pressure as output and gas-lift pressure as input. A transient window Z^N of length $N = 2000$ (around $k \approx 1.0 \times 10^5$ in Figure 10, the sampling time was $T_s = 1$ min) was used, which corresponds to 33.3 hours of operation. The six regressors that compose the model were chosen from a set of 220 candidate terms using the ERR (Billings et al., 1989) (see Sec. 4.1) and term clustering (Aguirre and Billings, 1995b). Parameters were estimated using orthogonal extended least squares. This resulted in a set of models with similar performance on validation data. Based on the principle of parsimony, the simpler model was retained (Aguirre et al., 2017).

It is important to notice that the identification data being around $k \approx 1.0 \times 10^5$ in Figure 10 means that they were measured when the process was operating roughly in the range of downhole pressure 75–80 kgf/cm². Over that range, the static nonlinearity of the model is quite consistent with the steady-state data (see Figure 11). Right after the identification window the process operate over a month (34 days) around 85 kgf/cm² slugging from 80 to 90 kgf/cm². After this, operation reduced the pressure gradually to levels as low as 70 kgf/cm². Around this point the process static behavior is quite different from that in the identification window. Hence it is no surprise that the black-box model is unable to correctly reproduce such a behavior at low pressure values.

One way around this problem is by means of grey-box modeling, as discussed in Section 7. Hence steady-state data over a wide range of operating points were taken from the historical records by computing the time average

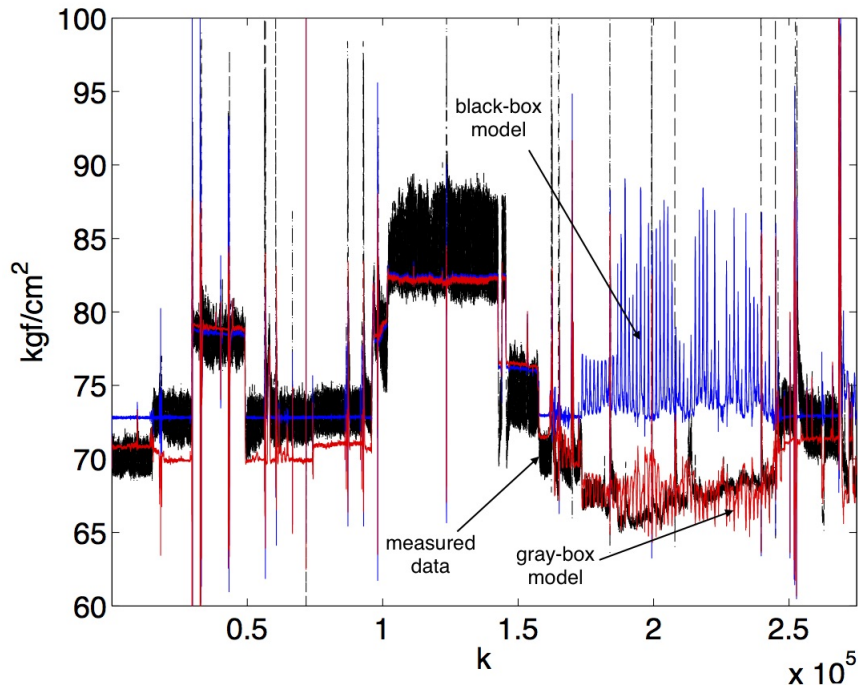


Figure 10: Black is the measured downhole pressure, blue is the output of a black-box polynomial model and red is the response of a grey-box polynomial model. See (Aguirre et al., 2017) for details.

over long windows of data whenever the process operated at a single point. Some of the averaged steady-state data are shown in Figure 11. Now using such data *simultaneously* with the original dynamical data, grey-box models were estimated by means of constrained estimation (see Section 7). As a consequence, the resulting models have the dynamics underlying the original data set Z^N which is roughly in the range 75–80 kgf/cm² and the static behavior of the data in Figure 11. The performance of one of such models against the black-box model is shown in Figure 10, which corresponds to over six months of operation. The benefits of using steady-state data in this nontrivial example is evident.

Similar results have been reported for neural networks (Aguirre et al., 2017) as shown in Figure 12.

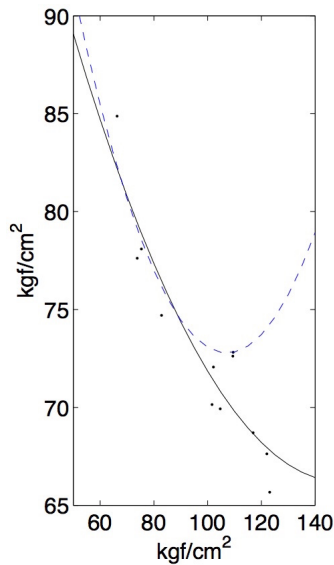


Figure 11: The dots indicate steady state data: x -axis is gas-lift pressure and y -axis is downhole pressure. The (black) solid line is a second order polynomial estimated from the data which ideally should be closely followed by that of estimated models. The blue dashed curve corresponds to the static characteristic of a black-box polynomial model which is only accurate in the range of the dynamical data (around 80 kgf/cm²). See (Aguirre et al., 2017) for details.

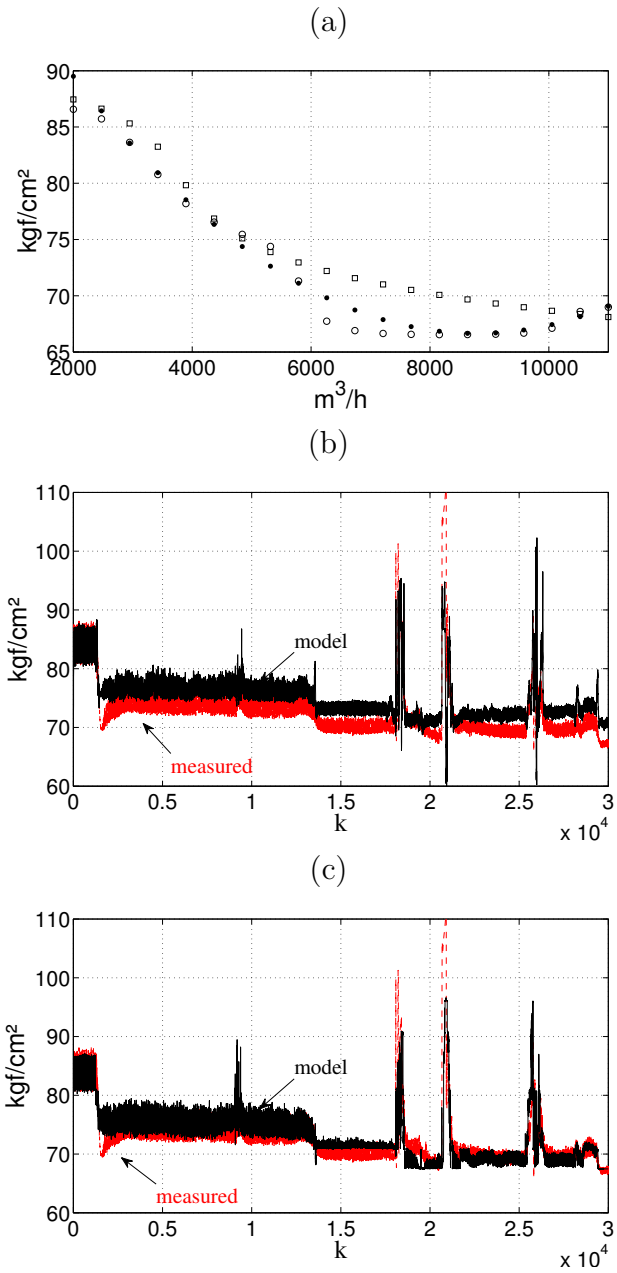


Figure 12: (a) Static curves (gas-lift flow *versus* downhole pressure), (\bullet) desired, (\square) black-box model and (\circ) grey-box model; downhole pressure prediction over validation data using Neural Networks: (b) black-box model and (c) grey-box-model (Freitas, 2013).

8.3 Imposing equilibria to model vector fields

This case study has been developed in cooperation with Rafael dos Santos (Santos, 2018) and Guilherme Pereira (Santos et al., 2018).

8.3.1 The challenge

An interesting problem in robotics is that of programming a robot to reach a certain location or position. A basic way of achieving this is to provide a trajectory to be followed. How to define which trajectory to provide for the robot is another issue. An elegant alternative is not to provide a trajectory itself but rather to provide a vector field for which infinite trajectories can be obtained, one for each possible initial condition. Hence, a vector field can be seen as a trajectory-producing mechanism. However for the resulting “solution” to be a useful trajectory it must end at the target. Traducing this in nonlinear dynamics language, the target must be a stable fixed point and the initial conditions must be taken within the corresponding basin of attraction. This is illustrated in Figure 13 where any initial condition taken in the green area will result in a trajectory that will eventually converge to the attractor, shown as a green circle. A set of trajectories that start at a set of neighbouring initial conditions are shown. Initial conditions taken in the white region will diverge to some other part of the state space.

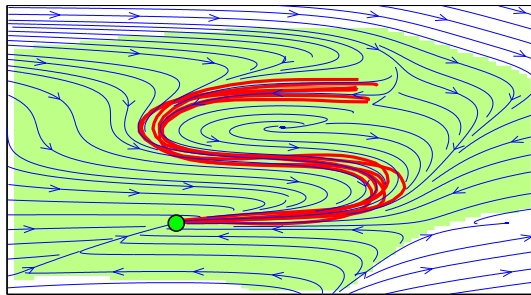


Figure 13: The vector field is represented by the blue lines with arrows. A set of possible trajectories are shown in red. The green region is the basin of attraction of the target, indicated by the green circle (Santos et al., 2018).

The goal in this case study is to identify from data a model for the vector field. Hence, such a model can be used to produce trajectories for the robot to follow. The first question we should ask is where do the data come

from. In this class of problems the data come from demonstrations, that is, a “teacher” (usually a human) performs a set of valid trajectories which are recorded and used as identification data (Fig. 14).

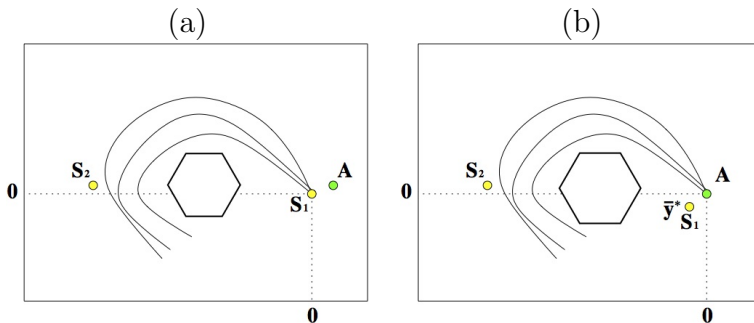


Figure 14: Three trajectories provided by the teacher. All the trajectories should finish at the target A that must be a stable fixed point of the resulting vector field (see text for details). In providing the trajectories, the teacher can, for instance, avoid obstacles, indicated here by the polygon. S_2 is a saddle that is not used in the example. Typical scenarios for (a) black-box techniques, and (b) grey-box methods. In (b) the *location* of S_1 was imposed, that is $S_1 = \bar{\mathbf{y}}^* = [y_1^*, y_2^*]^T$ is the new position of S_1 , and the origin remains a fixed point. The stability type of S_1 and A did not change. See text and (Santos et al., 2018) for details.

A central point in this problem can be stated as a question: is it guaranteed that the identified model will have a single attractor and that it will appear exactly at the meeting point of the trajectories? This question has a double answer. If the identification follows a black-box procedure, then the answer is negative (Fig. 14a). However, using grey-box techniques it is possible to guarantee that the model will satisfy the design requirements (Fig. 14b). This will be briefly detailed in what follows. Further details can be found in (Santos et al., 2018).

8.3.2 The methodology

For the sake of simplicity, the 2D will be described. The formulation for higher-order systems is straightforward although the implementation could become infeasible for such systems (Santos et al., 2018).

Given a set of n demonstrations $\mathbf{Y}_{(n)}$, which are trajectories in a state space \mathbb{R}^2 , the aim is to estimate NAR models that will approximate the vector field of which $\mathbf{Y}_{(n)}$ are integral curves. In this case, $\mathbf{y}(k) = [y_1(k) \ y_2(k)]^T$,

where $y_1(k)$ and $y_2(k)$ are the coordinates in \mathbb{R}^2 . Hence we search for models composed of 2 first-order difference equations, to produce $\hat{y}_1(k), \hat{y}_2(k)$.

The pool of candidate regressors is composed by all possible combinations up to degree ℓ of such variables plus a constant term. The regressors of each model equation are automatically chosen using the ERR criterion (see Eq. 5) together with Akaike's criterion (Akaike, 1974). A typical model has the general form:

$$\begin{aligned} y_1(k) &= F_1^\ell[y_1(k-1), y_2(k-1)] + e_1(k) \\ y_2(k) &= F_2^\ell[y_1(k-1), y_2(k-1)] + e_2(k) \end{aligned} \quad (45)$$

Assuming the model is stable, in steady-state $y_1(k) = y_1(k-1) = \bar{y}_1$; $y_2(k) = y_2(k-1) = \bar{y}_2$ and dropping the noise, the equilibria of model (45) – called fixed points – are given by (\bar{y}_1, \bar{y}_2) that are the solutions to the set of equations:

$$\begin{aligned} \bar{y}_1 &= F_1^\ell[\bar{y}_1, \bar{y}_2] \\ \bar{y}_2 &= F_2^\ell[\bar{y}_1, \bar{y}_2] \end{aligned} \quad (46)$$

and the stability of such fixed points can be determined by the eigenvalues λ_1, λ_2 of the Jacobian matrix

$$DF(\mathbf{y}) = \begin{bmatrix} \frac{\partial F_1^\ell}{\partial y_1(k-1)} & \frac{\partial F_1^\ell}{\partial y_2(k-1)} \\ \frac{\partial F_2^\ell}{\partial y_1(k-1)} & \frac{\partial F_2^\ell}{\partial y_2(k-1)} \end{bmatrix} \quad (47)$$

evaluated at such fixed points. The hyperbolic fixed point can be classified as: an *attractor* if $|\lambda_i| < 1, \forall i = 1, 2, \dots, p$; a *repellor* if $|\lambda_i| > 1, \forall i = 1, 2, \dots, p$; and a *saddle* if there are eigenvalues inside and outside the unit circle. A fixed point will be indicated by $\bar{\mathbf{y}}^*$.

As said before, if black-box techniques are used, typically the resulting vector field will not have a fixed point at the origin. This can be forced upon the model by removing the constant term of the pool of candidate regressors (Aguirre and Mendes, 1996). Unfortunately, although a fixed-point will appear at the origin by imposition, we cannot guarantee that it will be an attractor, as a matter of fact it will usually be a saddle. The good news is that because the demonstrations in $\mathbf{Y}_{(n)}$ all converge to the target,

the estimated vector field usually has an attractor slightly off the origin. This can be understood as a “perturbed” version of the ideal solution where the perturbations come from the imperfections of the trajectories, that are provided not by a vector field but rather by a human teacher.

A way of circumventing this problem is then to impose a fixed point nearby the origin. In doing so, this new equilibria will retain its type (a saddle in this example) and the origin becomes an attractor, as desired. Some details are provided in what follows. In order to impose that the model (45) should have a fixed point $\bar{\mathbf{y}}^* = [\bar{y}_1, \bar{y}_2]^T$, a constraint of the form $\mathbf{c} = S\boldsymbol{\theta}$ with

$$\mathbf{c} = \begin{bmatrix} \bar{y}_1 \\ \bar{y}_2 \end{bmatrix}, \quad S = \begin{bmatrix} F_1^\ell[\bar{y}_1, \bar{y}_2] \\ F_2^\ell[\bar{y}_1, \bar{y}_2] \end{bmatrix} \quad (48)$$

should be satisfied. This can be achieved using the estimator (17), as mentioned before.

Let us call \mathcal{M} an unconstrained model estimated from the data $\mathbf{Y}_{(n)}$ which has a fixed point at $\bar{\mathbf{y}}_1^*$. The parameters can be estimated anew from the same data using (17) with (48) in order to impose a new fixed point at $\bar{\mathbf{y}}^*$. The constrained model is referred to as \mathcal{M}_c . It has been conjectured that the fixed point $\bar{\mathbf{y}}^*$ of \mathcal{M}_c will be of the same type as that of $\bar{\mathbf{y}}_1^*$ of \mathcal{M} for sufficiently small $|\bar{\mathbf{y}}_1^* - \bar{\mathbf{y}}^*|$ (Santos et al., 2018).

This procedure has been performed for a whole library of demonstrations (available on the Web) and described in (Santos et al., 2018). A single example is given below for the sake of illustration.

The starting point is the set of demonstrations shown in red in Figure 15a and the blue lines illustrate the vector field of a black-box model. As it can be seen, the fixed point at the origin is a saddle, and there is an attractor slightly to the right. Using the grey-box techniques described, a fixed-point is imposed very close (to the left) of the origin, see Figure 15b. When parameters are estimated again, the origin becomes the attractor. It is as if the saddle, originally located at the origin, would shift to the left where the new fixed-point is imposed, and the attractor, originally to the right, would take residence at the origin which is guaranteed to be an equilibria by proper structure selection (Aguirre and Mendes, 1996). The model estimated using

grey-box techniques is:

$$\begin{aligned}
y_1(k) = & +0.983506 y_1(k-1) + 0.096590 y_2(k-1) \\
& -0.000078 y_1(k-1)^3 + 0.005253 y_2(k-1)^2 \\
& -0.000538 y_2(k-1)^3 - 0.016513 y_1(k-1) y_2(k-1) \\
& -0.000300 y_1(k-1)^2 y_2(k-1) - 0.004126 y_1(k-1)^2 \\
y_2(k) = & +0.779775 y_2(k-1) - 0.000042 y_1(k-1)^3 \\
& -0.015285 y_1(k-1) y_2(k-1) - 0.002493 y_2(k-1)^2 \\
& -0.000216 y_1(k-1)^2 y_2(k-1) - 0.004130 y_1(k-1) \\
& -0.000102 y_2(k-1)^3 - 0.001130 y_1(k-1)^2 \\
& +0.000001 y_1(k-1) y_2(k-1)^2.
\end{aligned} \tag{49}$$

Figure 15c shows in black some model-produced trajectories, which have all the same type of behavior than the original demonstrations produced by the human teacher. It should be noted that a great variety of trajectories can be produced by taking initial conditions from other regions in \mathbb{R}^2 within the basin of attraction.

This procedure has been successfully applied to a small mobile robot and to a Comau Smart Six manipulator. Details can be found in (Santos, 2018) and in the videos available at <https://goo.gl/AqMLAH>.

8.3.3 Benchmarks

To conclude this section, some pointers will be given for those who are interested in benchmarks and datasets.

The effort and initiative of Maarten Schoukens and Jean-Philippe Noël is worth pointing out (Schoukens and Noël, 2017). The website <https://www.nonlinearbenchmark.org> should be checked out (Schoukens and Noël, 2016).

Some of the data sets used by the author in his papers are freely available, as listed below:

1. chaotic data from Chua's circuit (Aguirre et al., 1997):
https://www.researchgate.net/publication/319493329_ChuaData1
2. data from a buck converter (Aguirre et al., 2000):
https://www.researchgate.net/publication/265412913_Measured_Data_of_Buck_Converter

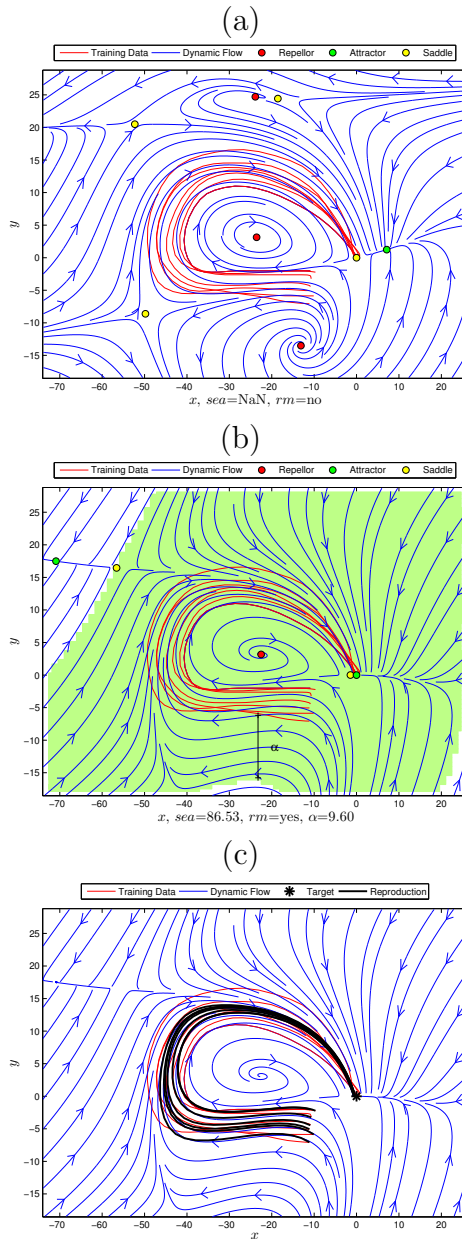


Figure 15: (a) The set of teacher-produced demonstrations is shown in red and the blue lines illustrate the vector field of a black-box model. (b) Result of the use of grey-box techniques, notice that now the origin is an attractor with its basing of attraction shown as the green area. (c) Different initial conditions are used to produce new model-generated trajectories (in black) using (49). See text and (Santos et al., 2018) for details.

3. data from a control valve ([Aguirre, 2014](#)):
https://www.researchgate.net/publication/263334571_DeadZoneValveData_RG
4. dynamical and static data from a heater ([Aguirre et al., 2002, 2005a](#)):
https://www.researchgate.net/publication/260177982_estat3
https://www.researchgate.net/publication/260177701_DIN3
https://www.researchgate.net/publication/260177800_Din4

9 Further Reading

There is a wealth of books that deal with system identification. Most books cover the theory related to linear systems. Early examples include ([Eykhoff, 1974](#); [Hsia, 1977](#)). A more modern approach with a view to prediction error methods is given by ([Norton, 1986](#); [Söderström and Stoica, 1989](#); [Ljung, 1999](#)). A text devoted to recursive techniques is ([Ljung and Söderström, 1983](#)). Nonlinear techniques are discussed in more recent texts ([Nelles, 2000](#); [Billings, 2013](#)).

Interesting discussions about the effects of the input on the parameter estimation process can be found in ([Bazanella et al., 2008](#); [Gevers et al., 2009](#)). In a different vein, Singh and co-workers have investigated the design of training and validating data sets from historical data ([Singh et al., 2019](#)).

Nepomuceno and Martins have endeavoured to establish a lower bound for free-run simulation errors of polynomial NARMAX models with chaotic dynamics ([Nepomuceno and Martins, 2016](#)). Nepomuceno has also investigated the use of multiobjective optimization techniques for determining the number of nodes of random neural networks ([Nepomuceno, 2019](#)). Hafiz and co-workers have used evolutionary techniques to solve multiobjective optimization problems related to structure selection of NARX polynomial models ([Hafiz et al., 2020a,b](#)). Related to this, an extensive review on probably the most popular algorithms based on computational intelligence to solve optimization problems related to parameter estimation and system identification has been provided in ([Quaranta et al., 2020](#)).

Bayma and co-workers proposed a way of analyzing identified NARX polynomial models in the frequency domain, by means of nonlinear output frequency response functions ([Bayma et al., 2018](#)). Ferreira and co-workers proposed the simultaneous use of the normalized RMSE, a coherence-based

index and the fourth-order cross-cumulant index. Such indices are combined to form a scale for model validation (Ferreira et al., 2017).

An interesting approach to the identification of nonlinear systems is the use of piecewise ARX models, where not only the model parameters but also the model space partitions must be estimated according to some optimality criterion (Barbosa et al., 2018). In a similar vein, but using neural-fuzzy models, Liu and co-workers besides the local model parameters and the location of the model partitions, they also estimate the number of partitions (Liu et al., 2019). Similar problems have been investigated by Barreto and co-workers using self organizing maps and K nearest neighbors algorithms to partition the data (Souza Junior et al., 2015; Barreto and Souza, 2016). In particular, in (Souza Junior et al., 2015) the concept of regional models is used as a model class which falls between global and local models. A similar approach which is not limited to local linear models is the Switched NARX or SNARX models. The challenge of defining the partitions (switching pattern) and structure selection of the local models has been addressed by Federico Bianchi and co-workers (Bianchi et al., 2020, 2021).

Early works on grey-box system identification in the sense treated in this paper include (Eskinat et al., 1993; Tulleken, 1993; Bohlin, 1994; Johansen, 1996).

Ribeiro and co-workers have provided insights into the trade-off between the smoothness of the cost function and i) the memory retention capabilities during training of neural networks (Ribeiro et al., 2019), and ii) the window over which the power of free-run simulation errors is minimized (Ribeiro et al., 2020).

The use of prior information in the context of neural networks is somewhat more involved. Some early results have been reported in (Thompson and Kramer, 1994; Amaral, 2001; Aguirre et al., 2004b; Li and Peng, 2006; Freitas, 2013). Grey-box identification techniques for radial basis function (RBF) networks has been addressed in (Aguirre et al., 2004b, 2007; Chen et al., 2011).

Barbosa et al. (2011) used the uncertainty related to sensor data to choose models from the Pareto set in biobjective optimization. A number of model structures were compared, including neural networks using data from hydraulic pumping system. Also, two different cost functions related to the dynamical data set were used one at a time: the conventional $J(Z, Z_{\mathcal{M}_1})$ which results in a convex optimization problem and $J(Z, Z_{\mathcal{M}_s})$, which results in a nonconvex optimization problem, that was solved using genetic

algorithms. The objective related to static data was always $J(Z_{\text{ss}}, Z_{\mathcal{M}_{\text{ss}}})$.

The use of biobjective estimation has been used to handle model uncertainty in the parameters (Teixeira and Aguirre, 2011) and in the model structure (Barbosa et al., 2015). As a matter of fact, the problem of characterizing and dealing with structural uncertainty remains an open problem that has attracted attention (Baldacchino et al., 2013; Gu and Wei, 2018). A biobjective cost function was used in (Mavkov et al., 2020) in the context of neural network training. The second objective did not convey any auxiliary information as such, but was used as a regularization term.

In (Wu et al., 2020) two different data sets are used to train two submodels. The combination of the outputs of both submodels form the final output. The parameters are estimated by minimizing a multiobjective cost function that penalizes the error of the final model, the difference between the submodel outputs and the number of parameters.

Using the evidences of symmetry in the dynamics of the solar dynamo (Letellier et al., 2006), the time series of the sunspots was mapped unto a symmetric space where it was possible to build models – that used symmetry as auxiliary information – to forecast the time series (Aguirre et al., 2008a).

Wei and Billings have discussed the modeling of COVID-19 dynamics and aspects of interpretability of NARMAX models (Wei and Billings, 2021). In this interesting application the use of large lags for both input and output, due to the delays associated with the pandemic dynamics, seem to be a keep aspect of the modeling. An interpretation of the use of large lags related to cyclical data has been put forward in (Aguirre et al., 2008b).

Acknowledgements

Financial support by CNPq and FAPEMIG (Brazil) is gratefully acknowledged. The careful reading of this manuscript by Petrus Abreu is acknowledged with thanks.

References

- Abreu, P. E. O. G. B., Tavares, L. A., Teixeira, B. O. S., and Aguirre, L. A. (2020). Identification and nonlinearity compensation of hysteresis using NARX models. *Nonlinear Dynamics*, 102(1):285–301.

- Aguirre, L. A. (1994). Term clustering and the order selection of linear continuous systems. *J. Franklin Inst.*, 331B(4):403–415.
- Aguirre, L. A. (1995). A nonlinear correlation function for selecting the delay time in dynamical reconstructions. *Phys. Lett.*, 203A(2,3):88–94.
- Aguirre, L. A. (1997). Recovering map static nonlinearities from chaotic data using dynamical models. *Physica D*, 100(1,2):41–57.
- Aguirre, L. A. (2014). Identification of smooth nonlinear dynamical systems with non-smooth steady-state features. *Automatica*, 50:1160–1166.
- Aguirre, L. A., Alves, G. B., and Corrêa, M. V. (2007). Steady-state performance constraints for dynamical models based on RBF networks. *Engineering Applications of Artificial Intelligence*, 20:924–935.
- Aguirre, L. A., Barbosa, B. H. G., and Braga, A. P. (2010). Prediction and simulation errors in parameter estimation for nonlinear systems. *Mechanical Systems and Signal Processing*, 24(8):2855–2867.
- Aguirre, L. A., Barroso, M. F. S., Saldanha, R. R., and Mendes, E. M. A. M. (2004a). Imposing steady-state performance on identified nonlinear polynomial models by means of constrained parameter estimation. *Proc. IEE Part D: Control Theory and Applications*, 151(2):174–179.
- Aguirre, L. A. and Billings, S. A. (1994). Validating identified nonlinear models with chaotic dynamics. *Int. J. Bifurcation and Chaos*, 4(1):109–125.
- Aguirre, L. A. and Billings, S. A. (1995a). Dynamical effects of overparametrization in nonlinear models. *Physica D*, 80(1,2):26–40.
- Aguirre, L. A. and Billings, S. A. (1995b). Improved structure selection for nonlinear models based on term clustering. *Int. J. Control*, 62(3):569–587.
- Aguirre, L. A., Coelho, M. C. S., and Corrêa, M. V. (2005a). On the interpretation and practice of dynamical differences between Hammerstein and Wiener models. *Proc. IEE Part D: Control Theory and Applications*, 152(4):349–356.
- Aguirre, L. A., Corrêa, M., and Cassini, C. C. S. (2002). Nonlinearities in NARX polynomial models: representation and estimation. *Proc. IEE Part D: Control Theory and Applications*, 149(4):343–348.

- Aguirre, L. A., Donoso-Garcia, P. F., and Santos-Filho, R. (2000). Use of *a priori* information in the identification of global nonlinear models — A case study using a Buck converter. *IEEE Trans. Circuits Syst. I*, 47(7):1081–1085.
- Aguirre, L. A. and Furtado, E. C. (2007). Building dynamical models from data and prior knowledge: the case of the first period-doubling bifurcation. *Physical Review E*, 76(046219).
- Aguirre, L. A., Furtado, E. C., and Tôrres, L. A. B. (2006). Evaluation of dynamical models: Dissipative synchronization and other techniques. *Physical Review E*, 74(066203).
- Aguirre, L. A. and Jácome, C. R. F. (1998). Cluster analysis of NARMAX models for signal-dependent systems. *Proc. IEE Part D: Control Theory and Applications*, 145(4):409–414.
- Aguirre, L. A., Letellier, C., and Maquet, J. (2008a). Forecasting the time series of sunspot numbers. *Solar Physics*, 249(1):103–120, DOI: 10.1007/s11207-008-9160-5.
- Aguirre, L. A., Lopes, R. A. M., Amaral, G., and Letellier, C. (2004b). Constraining the topology of neural networks to ensure dynamics with symmetry properties. *Physical Review E*, 69(026701).
- Aguirre, L. A. and Mendes, E. M. A. M. (1996). Nonlinear polynomial models: Structure, term clusters and fixed points. *Int. J. Bifurcation and Chaos*, 6(2):279–294.
- Aguirre, L. A., Rodrigues, D. D., Lima, S. T., and Martinez, C. B. (2008b). Dynamical prediction and pattern mapping in short term load-forecasting. *International Journal of Electrical Power & Energy Systems*, 30:73–82.
- Aguirre, L. A. and Rodrigues, G. G. (2012). Imposing a Hopf bifurcation on a model estimated from noisy data from the delayed logistic equation. In *Proceedings of the Third IFAC-CHAOS Conference*, pages 12–17, Cancun, Mexico.
- Aguirre, L. A., Rodrigues, G. G., and Mendes, E. M. A. M. (1997). Nonlinear identification and cluster analysis of chaotic attractors from a real implementation of Chua’s circuit. *Int. J. Bifurcation and Chaos*, 7(6):1411–1423.
- Aguirre, L. A., Teixeira, B. O. S., Barbosa, B. H. G., Teixeira, A. F., Campos, M. C. M. M., and Mendes, E. M. A. M. (2017). Development of soft sensors for permanent downhole gauges in deepwater oil well. *Control Engineering Practice*, 65:83–99.

- Aguirre, L. A., Teixeira, B. O. S., and Tôrres, L. A. B. (2005b). Using data-driven discrete-time models and the unscented Kalman filter to estimate unobserved variables of nonlinear systems. *Physical Review E*, 72(026226).
- Akaike, H. (1974). A new look at the statistical model identification. *IEEE Trans. Automat. Contr.*, 19(6):716–723.
- Alves, M. A., Corrêa, M. V., and Aguirre, L. A. (2012). Use of self-consistency in the structure selection of NARX polynomial models. *Int. J. Modelling, Identification and Control*, 15(1):1–12.
- Alves, V. A. O., de Godoy, R. J. C., and Garcia, C. (2017). An innovative approach for optimal time delay estimation in system identification. *Journal of Control, Automation and Electrical Systems*, 28:429–443.
- Amaral, G. F. V. (2001). Use of prior information with neural networks for the identification of nonlinear dynamical systems (in portuguese). Master’s thesis, Programa de Pós-Graduação em Engenharia Elétrica, Universidade Federal de Minas Gerais.
- Araújo, I. B. Q., Guimarães, J. P. F., Fontes, A. I. R., Linhares, L. L. S., Martins, A. M., and Araújo, F. M. U. (2019). NARX model identification using correntropy criterion in the presence of non-gaussian noise. *Journal of Control, Automation and Electrical Systems*, 30:453–464.
- Avellina, M., Brankovic, A., and Piroddi, L. (2017). Distributed randomized model structure selection for NARX models. *International Journal of Adaptive Control and Signal Processing*, 31(12):1853–1870.
- Baeza, J. R. and Garcia, C. (2018). Friction compensation in pneumatic control valves through feedback linearization. *Journal of Control, Automation and Electrical Systems*, 29(3):303–317.
- Bai, E. W. (2002). A blind approach to the Hammerstein-Wiener model identification. *Automatica*, 38:967–979.
- Baldacchino, T., Anderson, S. R., and Kadiramanathan, V. (2013). Computational system identification for bayesian narmax modelling. *Automatica*, 49(9):2641–2651.
- Ballini, R. and Gomide, F. (2002). Heuristic learning in recurrent neural fuzzy networks. *Journal of Intelligent & Fuzzy Systems*, 13(2-4):63–74.

- Barbosa, A. M., Takahashi, R. H. C., and Aguirre, L. A. (2015). Equivalence of non-linear model structures based on pareto uncertainty. *IET Control Theory & Applications*, 9(16):2423–2429.
- Barbosa, B. H. G., Aguirre, L. A., and Braga, A. P. (2018). Piecewise affine identification of a hydraulic pumping system using evolutionary computation. *IET Control Theory & Applications*.
- Barbosa, B. H. G., Aguirre, L. A., Martinez, C. B., and Braga, A. P. (2011). Black and gray-box identification of a hydraulic pumping system. *IEEE Trans. Control Technology*, 19(2):398–406.
- Barreto, G. A. and Souza, L. G. M. (2016). Novel approaches for parameter estimation of local linear models for dynamical system identification. *Applied Intelligence*, 44:149–165.
- Barroso, M. S. F., Takahashi, R. H. C., and Aguirre, L. A. (2007). Multi-objective parameter estimation via minimal correlation criterion. *J. Proc. Cont.*, 17(4):321–332.
- Bayma, R. S., Zhu, Y., and Lang, Z.-Q. (2018). The analysis of nonlinear systems in the frequency domain using nonlinear output frequency response functions. *Automatica*, 94:452–457.
- Bazanella, A. S., Gevers, M., Miskovic, L., and Anderson, B. D. O. (2008). Iterative minimization of H_2 control performance criteria. *Automatica*, 44:2549–2559.
- Belkin, M., Hsu, D., Ma, S., and Mandal, S. (2019). Reconciling modern machine-learning practice and the classical bias-variance trade-off. *Proceedings of the National Academy of Sciences*, 116(32):15849–15854.
- Bernstein, D. S. (2007). Ivory ghost [ask the experts]. *IEEE Control Systems Magazine*, 27(5):16–17.
- Bianchi, F., Breschi, V., Piga, D., and Piroddi, L. (2021). Model structure selection for switched NARX system identification: A randomized approach. *Automatica*, 125:109415.
- Bianchi, F., Falsone, A., Prandini, M., and Piroddi, L. (2017). A randomised approach for NARX model identification based on a multivariate bernoulli distribution. *Int. J. of Systems Science*, 48(6):1203–1216.

- Bianchi, F., Prandini, M., and Piroddi, L. (2020). A randomized two-stage iterative method for switched nonlinear systems identification. *Nonlinear Analysis: Hybrid Systems*, 35:100818.
- Billings, S. A. (1980). Identification of nonlinear systems — a survey. *IEE Proceedings Pt. D*, 127(6):272–285.
- Billings, S. A. (2013). *Nonlinear System Identification: NARMAX Methods in the Time, Frequency, and Spatio-Temporal Domains*. Wiley.
- Billings, S. A. and Aguirre, L. A. (1995). Effects of the sampling time on the dynamics and identification of nonlinear models. *Int. J. Bifurcation and Chaos*, 5(6):1541–1556.
- Billings, S. A. and Chen, S. (1989). Identification of nonlinear rational systems using a predictor-error estimation algorithm. *Int. J. Systems Sci.*, 20(3):467–494.
- Billings, S. A. and Chen, S. (1992). Neural networks and system identification. In Warwick, K., Irwing, G. W., and Hunt, K. J., editors, *Neural Networks for Systems and Control*, chapter 9, pages 181–205. Peter Peregrinus, London.
- Billings, S. A., Chen, S., and Korenberg, M. J. (1989). Identification of MIMO nonlinear systems using a forward-regression orthogonal estimator. *Int. J. Control*, 49(6):2157–2189.
- Billings, S. A. and Tao, Q. H. (1991). Model validation tests for nonlinear signal processing applications. *Int. J. Control*, 54:157–194.
- Billings, S. A. and Zhu, Q. M. (1991). Rational model identification using an extended least-squares algorithm. *Int. J. Control*, 54(3):529–546.
- Billings, S. A. and Zhu, Q. M. (1994). Nonlinear model validation using correlation tests. *Int. J. Control*, 60(6):1107–1120.
- Billings, S. A. and Zhu, Q. M. (1995). Model validation tests for multivariable nonlinear models including neural networks. *Int. J. Control*, 62(4):749–766.
- Bittencourt, A. C., Isaksson, A. J., Peretzki, D., and Forsman, K. (2015). An algorithm for finding process identification intervals from normal operating data. *Processes*, 3:357–383.
- Bohlin, T. (1994). A case study of grey box identification. *Automatica*, 30(2):307–318.

- Bombois, X., Scorletti, G., Gevers, M., Van den Hof, P. M. J., and Hildebrand, R. (2006). Least costly identification experiment for control. *Automatica*, 42:1651–1662.
- Bonin, M., Seghezza, V., and Piroddi, L. (2010). NARX model selection based on simulation error minimisation and LASSO. *IET Control Theory and Applications*, 4(7):1157–1168.
- Borjas, S. D. M. and Garcia, C. (2011). Subspace identification for industrial processes. *TEMA Tend. Mat. Apl. Comput.*, 12:183–194.
- Brown, R., Rul'kov, N. F., and Tracy, E. R. (1994). Modeling and synchronizing chaotic systems from time-series data. *Phys. Rev. E*, 49(5):3784–3800.
- Campello, R. J. G. B., do Amaral, W. C., and Favier, G. (2006). A note on the optimal expansion of Volterra models using Laguerre functions. *Automatica*, 42:689–693.
- Chankong, V. and Haimes, Y. Y. (1983). *Multiobjective decision making: theory and methodology*. North-Holland, New York.
- Chen, S. and Billings, S. A. (1989). Representations of nonlinear systems: the NARMAX model. *Int. J. Control*, 49(3):1013–1032.
- Chen, S., Billings, S. A., Cowan, C. F. N., and Grant, P. M. (1990a). Practical identification of NARMAX models using radial basis functions. *Int. J. Control*, 52(6):1327–1350.
- Chen, S., Billings, S. A., and Grant, P. M. (1990b). Non-linear system identification using neural networks. *Int. Journal of Control*, 51(6):1191–1214.
- Chen, S., Hong, X., and Harris, C. J. (2011). Grey-box radial basis function modelling. *Neurocomputing*, 74(10):1564–1571.
- Chen, S., Wolfgang, A., Harris, C. J., and Hanzo, L. (2008). Symmetric rbf classifier for nonlinear detection in multiple-antenna-aided systems. *IEEE Trans. Neural Networks*, 19(5):737–745.
- Corrêa, M., Aguirre, L. A., and Saldanha, R. R. (2002). Using prior knowledge to constrain parameter estimates in nonlinear system identification. *IEEE Trans. Circuits Syst. I*, 49(9):1376–1381.
- Draper, N. R. and Smith, H. (1998). *Applied Regression Analysis, Third edition*. John Wiley and Sons, New York.

- Eskinat, E., Johnson, S. H., and Luyben, W. L. (1993). Use of auxiliary information in system identification. *Ind. Eng. Chem. Res.*, 32:1981–1992.
- Eykhoff, P. (1974). *System Identification - Parameter and State Estimation*. John Wiley and Sons.
- Falsone, A., Piroddi, L., and Prandini, M. (2015). A randomized algorithm for nonlinear model structure selection. *Automatica*, 60:227–238.
- Farina, M. and Piroddi, L. (2010). An iterative algorithm for simulation error based identification of polynomial input-output models using multi-step prediction. *Int. Journal of Control*, 83(7):1442–1456.
- Ferreira, D. D., Nepomuceno, E. G., Cerqueira, A. S., and Mendes, T. M. (2017). A model validation scale based on multiple indices. *Electrical Engineering*, 99:325–334.
- Forgione, M. and Piga, D. (2021). Continuous-time system identification with neural networks: Model structures and fitting criteria. *European Journal of Control*, 59:69–81.
- Freitas, L. (2013). Use of prior knowledge in neural networks and committees construction for dynamical systems identification (in portuguese). Master’s thesis, Programa de Pós-Graduação em Engenharia Elétrica, Universidade Federal de Minas Gerais.
- Geman, S., Bienenstock, E., and Doursat, R. (1992). Neural networks and the bias/variance dilemma. *Neural Computation*, 4(1):1–58.
- Gevers, M., Bazanella, A. S., Bombois, X., and Miskovic, L. (2009). Identification and the information matrix: How to get just sufficiently rich? *IEEE Transactions on Automatic Control*, 54(12):2828–2840.
- Göttsche, T. H., Hunt, K. J., and Johansen, T. A. (1998). Nonlinear dynamics modelling via operating regime decomposition. *Mathematics and Computers in Simulation*, 46:543–550.
- Gouesbet, G. and Letellier, C. (1994). Global vector field reconstruction by using a multivariate polynomial l_2 approximation on nets. *Phys. Rev. E*, 49(6):4955–4972.
- Gu, Y. and Wei, H. L. (2018). A robust model structure selection method for small sample size and multiple datasets problems. *Information Sciences*, 451:195–209.

- Hafiz, F., Swain, A., and Mendes, E. M. A. M. (2019). Two-dimensional (2D) particle swarms for structure selection of nonlinear systems. *Neurocomputing*, 367:114–129.
- Hafiz, F., Swain, A., and Mendes, E. M. A. M. (2020a). Multi-objective evolutionary framework for non-linear system identification: A comprehensive investigation. *Neurocomputing*, 386:257–280.
- Hafiz, F. M. F., Swain, A., Mendes, E. M. A. M., and Aguirre, L. A. (2020b). Multiobjective evolutionary approach to grey-box identification of buck converter. *IEEE Transactions on Circuits and Systems I*, 67(6):2016–2028.
- Haynes, B. R. and Billings, S. A. (1994). Global analysis and model validation in nonlinear system identification. *J. of Nonlinear Dynamics*, 5(1):93–130.
- Hong, X., Mitchell, R. J., Chen, S., Harris, C. J., Li, K., and Irwin, G. W. (2008). Model selection approaches for non-linear system identification: a review. *Int. J. Systems Sci.*, 39(10):925–946.
- Hsia, T. C. (1977). *System Identification*. Lexington Books.
- Johansen, T. A. (1996). Identification of non-linear systems using empirical data and prior knowledge - an optimization approach. *Automatica*, 32:337.
- Johansen, T. A. and Foss, B. A. (1993). Constructing NARMAX models using ARMAX models. *Int. J. Control*, 58(5):1125–1153.
- Khosravi, M. and Smith, R. S. (2021). Nonlinear system identification with prior knowledge on the region of attraction. *IEEE Control Systems Letters*, 5(3):1091–1096.
- Leontaritis, I. J. and Billings, S. A. (1985). Input-output parametric models for nonlinear systems part I: Deterministic nonlinear systems. *Int. J. Control*, 41(2):303–328.
- Leontaritis, I. J. and Billings, S. A. (1987a). Experimental design and identifiability for nonlinear systems. *Int. J. Systems Sci.*, 18(1):189–202.
- Leontaritis, I. J. and Billings, S. A. (1987b). Model selection and validation methods for non-linear systems. *Int. J. Control*, 45(1):311–341.
- Letellier, C., Aguirre, L. A., Maquet, J., and Gilmore, R. (2006). Evidence for low dimensional chaos in sunspot cycles. *Astronomy & Astrophysics*, 449:379–387.

- Letellier, C., Gouesbet, G., and Rulkov, N. F. (1996). Topological analysis of chaos in equivariant electronic circuits. *Int. J. Bifurcation and Chaos*, 6(12):2531–2555.
- Letellier, C., Le Sceller, L., Dutertre, P., Gouesbet, G., Fei, Z., and Hudson, J. L. (1995). Topological characterization and global vector field reconstruction from an experimental electrochemical system. *Journal of Physical Chemistry*, A99:7016–7027.
- Letellier, C., Ménard, O., and Aguirre, L. A. (2002). Validation of selected global models. In Soofi, A. S. and Cao, L., editors, *Modeling and Forecasting Financial Data: Techniques of Nonlinear Dynamics*, pages 283–302. Kluwer.
- Letellier, C., Mangiarotti, S., Sendiña-Nadal, I., and Rössler, O. (2018). Topological characterization versus synchronization for assessing (or not) dynamical equivalence. *CHAOS*, 28(045107).
- Li, K. and Peng, J. X. (2006). System oriented neural networks — problem formulation, methodology and application. *Int. J. of Pattern Recognition and Artificial Intelligence*, 20(2):143–158.
- Lindskog, P. and Ljung, L. (1995). Tools for semiphysical modelling. *International Journal of Adaptive Control and Signal Processing*, 9(6):509–523.
- Liu, Z., Fang, H., and Xu, J. (2019). Identification of piecewise linear dynamical systems using physically-interpretable neural-fuzzy networks: Methods and applications to origami structures. *Neural Networks*, 116:74–87.
- Ljung, L. (1999). *System Identification, Theory for the User*. Second Edition. Prentice Hall, New Jersey.
- Ljung, L. and Söderström, T. (1983). *Theory and practice of recursive identification*. MIT press, Cambridge, MA.
- Lu, S., Ju, K. H., and Chon, K. H. (2001). A new algorithm for linear and nonlinear ARMA model parameter estimation using affine geometry. *IEEE Trans. Biomed. Eng.*, 48(10):1116–1124.
- Mangiarotti, S., Coudret, R., Drapeau, L., and Jarlan, L. (2012). Polynomial search and global modeling: Two algorithms for modeling chaos. *Phys. Rev. E*, 86(4):046205.

- Martins, S. A. M. and Aguirre, L. A. (2016). Sufficient conditions for rate-independent hysteresis in autoregressive identified models. *Mechanical Systems and Signal Processing*, 75:607–617.
- Martins, S. A. M., Nepomuceno, E. G., and Barroso, M. F. S. (2013). Improve structure detection for polynomial NARX models using multiobjective error reduction ratio. *Journal of Control, Automation and Electrical Systems*, 24(6):764–772.
- Masri, S. F., Chassiakos, A. G., and Caughey, T. K. (1993). Identification of nonlinear dynamic systems using neural networks. *Transactions of the ASME, J. Appl. Mech.*, 60:123–133.
- Mavkov, B., Forgiione, M., and Piga, D. (2020). Integrated neural networks for nonlinear continuous-time system identification. *IEEE Control Systems Letters*, 4(4):851–856.
- Mendes, E. M. A. M. and Billings, S. A. (2001). An alternative solution to the model structure selection problem. *IEEE Trans. on Man and Cybernetics - Part A*, 36(21):597–608.
- Narendra, K. S. and Parthasarathy, K. (1990). Identification and control of dynamical systems using neural networks. *IEEE Transactions on Neural Networks*, 1:4–27.
- Nelles, O. (2000). *Nonlinear System Identification: From Classical Approaches to Neural Networks and Fuzzy Models*. Springer.
- Nepomuceno, E. G. (2019). A novel method for structure selection of the recurrent random neural network using multiobjective optimisation. *Applied Soft Computing Journal*, 76:607–614.
- Nepomuceno, E. G. and Martins, S. A. M. (2016). A lower bound error for free-run simulation of the polynomial NARMAX. *Systems Science & Control Engineering*, 4(1):50–58.
- Nepomuceno, E. G., Takahashi, R., Aguirre, L. A., Neto, O. M., and Mendes, E. M. A. M. (2004). Multiobjective nonlinear system identification: a case study with thyristor controlled series capacitor (TCSC). *ijss*, 35(9):537–546.
- Nepomuceno, E. G., Takahashi, R. H. C., and Aguirre, L. A. (2007). Multiobjective parameter estimation: Affine information and least-squares formulation. *Int. J. Control*, 80(6):863–871.

- Norton, J. P. (1986). *An Introduction to Identification*. Academic Press, London.
- Ogawa, S., Ikeguchi, T., Matozaki, T., and Aihara, K. (1996). Nonlinear modeling by radial basis function networks. *IEICE Trans. Fundamentals*, E79-A(10):1608–1617.
- Piroddi, L. (2008). Simulation error minimization methods for NARX model identification. *Int. J. Modelling, Identification and Control*, 3(4):392–403.
- Piroddi, L. and Spinelli, W. (2003). An identification algorithm for polynomial NARX models based on simulation error minimization. *Int. J. Control*, 76(17):1767–1781.
- Pittino, F., Diversi, R., Benini, L., and Bartolini, A. (2020). Robust identification of thermal models for in-production high-performance-computing clusters with machine learning-based data selection. *IEEE Trans. Computer-Aided Design of Integrated Circuits and Systems*, 39(10):2042–2054.
- Quaranta, G., Lacarbonara, W., and Masri, S. F. (2020). A review on computational intelligence for identification of nonlinear dynamical systems. *Nonlinear Dynamics*, 99:1709–1761.
- Reed, R. (1993). Pruning algorithms — A survey. *IEEE Trans. Neural Networks*, 4(5):740–747.
- Retes, P. F. L. and Aguirre, L. A. (2019). NARMAX model identification using a randomized approach. *Int. J. Modelling, Identification and Control*, 31(3):205–216.
- Ribeiro, A. H. and Aguirre, L. A. (2015). Selecting transients automatically for the identification of models for an oil well. In *Preprints of the 2nd IFAC Workshop on Automatic Control in Offshore Oil and Gas Production*, volume 48 of *IFAC-PapersOnLine*, pages 154–158.
- Ribeiro, A. H. and Aguirre, L. A. (2018). “Parallel training considered harmful?”: Comparing series-parallel and parallel feedforward network training. *Neurocomputing*, 316:222–231.
- Ribeiro, A. H., Hendriks, J. N., Wills, A. G., and Schön, T. B. (2021). Beyond Occam’s razor in system identification: Double-descent when modeling dynamics. *IFAC-PapersOnLine*, 54(7):97–102.

- Ribeiro, A. H., Tiels, K., Aguirre, L. A., and Schon, T. B. (2019). The trade-off between long-term memory and smoothness for recurrent networks. *arXiv:1906.08482v1 [cs.LG]*.
- Ribeiro, A. H., Tiels, K., Umenberger, J., Schön, T. B., and Aguirre, L. A. (2020). On the smoothness of nonlinear system identification. *Automatica*, 121(109158).
- Ricco, R. A. and Teixeira, B. O. S. (2021). Least-squares parameter estimation for state-space models with state equality constraints. *International Journal of Systems Science*, pages 1–13.
- Rocha, O. and Serra, G. (2017). Adaptive neuro-fuzzy black-box modeling based on instrumental variable evolving algorithm. *Journal of Control, Automation and Electrical Systems*, 28:50–67.
- Romano, R. A. and Garcia, C. (2011). Valve friction and nonlinear process model closed-loop identification. *Journal of Process Control*, 21(4):667–677.
- Santos, R. F. (2018). *Programação de Robôs por Demonstração Utilizando Modelos Não Lineares Autoregressivos*. PhD thesis, Programa de Pós-Graduação em Engenharia Elétrica da UFMG, Belo Horizonte, M.G., Brasil.
- Santos, R. F., Pereira, G. A. S., and Aguirre, L. A. (2018). Learning robot reaching motions by demonstration using nonlinear autoregressive models. *Robotics and Autonomous Systems*, 107:182–195.
- Schoukens, J., Wetwick, D., Ljung, L., and Dobrowiecki, T. (2021). Nonlinear system identification with dominant output noise – a case study on the silverbox. *IFAC-PapersOnLine*, 54-7:679–684.
- Schoukens, M. and Noël, J. P. (2016). Nonlinear system identification benchmarks. <https://www.nonlinearbenchmark.org/>.
- Schoukens, M. and Noël, J. P. (2017). Three benchmarks addressing open challenges in nonlinear system identification. *IFAC-PapersOnLine*, 50:446–451.
- Schoukens, M. and Tiels, K. (2017). Identification of block-oriented nonlinear systems starting from linear approximations: A survey. *Automatica*, 85:272–292.
- Singh, H., Pani, A. K., and Mohanta, H. K. (2019). Quality monitoring in petroleum refinery with regression neural network: Improving prediction accuracy with appropriate design of training set. *Measurement*, 134:698–709.

- Söderström, T. and Stoica, P. (1989). *System Identification*. Prentice Hall International, London.
- Souza Junior, A. H., Barreto, G. A., and Corona, F. (2015). Regional models: A new approach for nonlinear system identification via clustering of the self organizing map. *Neurocomputing*, 147:31–46.
- Stoica, P., Eykhoff, P., Janssen, P., and Söderström, T. (1986). Model structure selection by cross-validation. *International Journal of Control*, 43:1841–1878.
- Tavares, L. A., Abreu, P. E. O. G. B., and Aguirre, L. A. (2022). Nonlinearity compensation based on identified NARX polynomials models. *Nonlinear Dynamics*, 107:709–725.
- Teixeira, B. O. S. and Aguirre, L. A. (2011). Using uncertain prior knowledge to improve identified nonlinear dynamic models. *Journal of Process Control*, 21:82–91.
- Teixeira, B. O. S., Castro, W. S., Teixeira, A. F., and Aguirre, L. A. (2014). Data-driven soft sensor of downhole pressure for a gas-lift oil well. *Control Engineering Practice*, 22:34–43.
- Thompson, M. L. and Kramer, M. A. (1994). Modeling chemical processes using prior knowledge and neural networks. *Automatica*, 40(8):1328–1340.
- Tulleken, H. J. A. F. (1993). Grey-box modelling and identification using physical knowledge and bayesian techniques. *Automatica*, 29(2):285–308.
- Van Overschee, P. and De Moore, B. (1996). *Subspace Identification for Linear Systems*. Kluwer Academic.
- Wei, H. L. and Billings, S. A. (2008). Model structure selection using an integrated forward orthogonal search algorithm interfered with squared correlation and mutual information. *Int. J. Modelling, Identification and Control*, 3(4):341–356.
- Wei, H. L. and Billings, S. A. (2009). Improved parameter estimates for non-linear dynamical models using a bootstrap method. *Int. J. Control*, 82(11):1991–2001.
- Wei, H. L. and Billings, S. A. (2021). Modelling COVID-19 pandemic dynamics using transparent, interpretable, parsimonious and simulatable (TIPS) machine learning models: A case study from systems thinking and system identification perspectives. *medrxiv.org/content/10.1101/2021.11.01.21265653v1*.

- Wei, H. L., Billings, S. A., and Liu, J. (2004). Term and variable selection for non-linear system identification. *Int. J. Control*, 77(1):86–110.
- Wu, D., Ma, Z., Yu, S., and Zhu, Q. M. (2008). An enhanced back propagation algorithm for parameter estimation of rational models. *Int. J. Modelling, Identification and Control*, 5(1):27–37.
- Wu, X., Han, H., Liu, Z., and Qiao, J. (2020). Data-knowledge-based fuzzy neural network for nonlinear system identification. *IEEE Trans. on Fuzzy Systems*, 28(9):2209–2221.
- Young, P. C. (1970). An instrumental variable method for real-time identification of a noisy process. *Automatica*, 6(2):271–287.
- Zhu, Q. M. and Billings, S. A. (1993). Parameter estimation for stochastic nonlinear rational models. *Int. J. Control*, 57(2):309–333.
- Zhu, Q. M., Zhang, L. F., and Longden, A. (2007). Development of omnidirectional correlation functions for nonlinear model validation. *Automatica*, 43:1519–1531.